waternet
waterschap amstel gooi en vecht
gemeente amsterdam

Universiteit Utrecht

Modelling the removal of microorganisms by slow sand filtration

Master thesis

Erik Vissink

Student number: 3649962

Master: Earth, Surface and Water

Supervisors:

Prof. Jack Schijven (UU, RIVM)
René van der Aa (Waternet)
Yolanda Dullemont (Waternet)

26-09-2016

Index

Abstract

Slow sand filtration (SSF) is used for the removal of pathogenic microorganisms during drinking water production. The Dutch government has a drinking water policy, which includes an infection risk limit of 1 infection per 10,000 persons per year. Therefore, the concentrations of microorganism in the drinking water have to be determined. The microorganism concentrations in the influent as well as in the effluent water of SSF are in most cases below the detection limit. A model was developed by the RIVM, which calculates the removal efficiency of SSF under different conditions. This model was developed based on the data from pilot-scale experiments, which use indicator organisms in concentrations far above the detection limit.

We obtained a better understanding of the influence of the Schmutzdecke on the head loss in the full-scale slow sand filters. A correction of the head loss was conducted for the parameters discharge and water temperature. With this correction we obtained a corrected head loss which is solely influenced by the Schmutzdecke. Most of the full-scale filters showed a seasonal dependent development of the corrected head loss. The seasonal fluctuation could be caused by temperature dependent predation rates. Moreover, the value of the initial corrected head loss is related to the rate of head loss increase. A small part of the full-scale filters did not have a significant corrected head loss increase. This could be due to tunnel forming worms, *Eisenia* (*annelids*).

To improve the current model for the removal of microorganisms, some adjustments to this model are conducted. No relation was found between the removal of microorganisms and the head loss. There was a relation found of the sticking efficiency with the grain size and the water velocity. This was ascribed to the ratio of available surface sites which are favourable for attachment. The sticking efficiency was correlated to the grain size to the power of 2.5 and inversely correlated to the water velocity to the power of 2.9; $\alpha = F2 * dc^{2.5} / v^{2.9}$. Where F2 is the sticking factor, which is 0.0037 for *E.coli* and 0.00022 for MS2. With these new insights, we changed the location specific model to an universal model for all locations. This new model has a very strong dependency on the water velocity compared to the reference model. Besides, there is a different dependency on the grain size compared with the reference model. A smaller grain size is not always better according to the removal for the new model.

Samenvatting

Langzame zandfiltratie (LZF) wordt toegepast om pathogene micro-organismen te verwijderen bij de productie van drinkwater. The Nederlandse overheid hanteert een beleid waarbij het infectierisico van 1 op de 10,000 personen per jaar niet mag worden overschreden. Daarvoor moeten de concentraties in het drinkwater worden bepaald. The concentraties in de inname en de afvoer van de LZF zijn meestal onder de detectiegrens. Een model is ontwikkeld door het RIVM, waarbij het verwijderingsrendement van LZF wordt berekend onder verschillende bedrijfscondities. Dit model is ontwikkeld op basis van doseerproeven, waarbij indicatieorganismen worden gebruikt in een concentratie ver boven het detectie limiet.

Wij hebben een beter inzicht gekregen in het effect van de Schmutzdecke op de ontwikkeling van de bedweerstand in de productiefilters. Er is een correctie gedaan op de bedweerstand voor het debiet en de watertemperatuur. Met deze correctie is een gecorrigeerde bedweerstand verkregen, die alleen afhankelijk is van de ontwikkeling van de Schmutzdecke. De meeste productiefilters hebben een seizoensafhankelijke ontwikkeling. Deze ontwikkeling zou kunnen komen door een seizoensafhankelijke predatiesnelheid. Daarnaast is de initiële waarde van de gecorrigeerde bedweerstand van invloed op de stijging van de gecorrigeerde bedweerstand. Een klein deel van de productie filters hebben geen verhoging van de gecorrigeerde bedweerstand. Dit is mogelijk toe te schijven aan tunnel makende wormen, *Eisenia* (*annalids*).

Om het huidige verwijderingsmodel te verbeteren, hebben we een aantal veranderingen toegepast op het model. Er is geen relatie gevonden tussen de bedweerstand en de verwijdering van micro-organismen. Er is wel een relatie gevonden tussen de *sticking* efficiency (α) en zowel de korrelgrootte als de watersnelheid. De *sticking efficiency* is gecorreleerd aan de korrelgrootte tot de macht 2.5 en invers gecorreleerd aan de watersnelheid tot de macht 2.9; $\alpha = F2 * dc^{2.5} / v^{2.9}$. De F2 is de *sticking factor* en heeft een waarde van 0.0037 voor *E.coli* en 0.00022 voor MS2. Met deze nieuwe inzichten, is het locatie specifieke model verandert in een universeel model, die voor elke locatie toegepast kan worden. Het nieuwe model is sterk afhankelijk van de watersnelheid in vergelijk met het referentiemodel. Daarnaast, is er ook een andere afhankelijkheid van de korrelgrootte in vergelijking met het referentie. Een kleinere korrelgrootte is niet altijd beter voor de verwijdering volgens het nieuwe model.

1. Introduction

Slow sand filtration (SSF) is often the last treatment step in the production of drinking water from surface water sources in the Netherlands. It effectively removes pathogenic microorganisms from the influent water. The Dutch government has a drinking water policy, which includes an infection risk limit of 1 infection per 10.000 persons per year. To demonstrate that this limit will not be exceeded, the pathogenic and indicator microorganism concentrations in the raw water are examined. Also the indicator microorganism concentrations before and after each treatment step are examined. The latter is need to determine the removal efficiency of every treatment step. The microorganism concentrations in the influent as well as in the effluent water of full-scale SSF are in most cases below the detection limit. Therefore, a model was developed by the RIVM, which calculates the removal efficiency of SSF under different conditions (Schijven et al. 2013). This model has been developed using the data from pilot-scale experiments, in which indicator organisms were seeded in concentrations far above the detection limit. Bacteriophage MS2 is used as indicator organism for viruses and *E.coli* WR1 is used as indicator organism for bacteria (Anonymous, 2005).

The current model includes the physical conditions: grain size, size of the organism, water temperature, water velocity, porosity and the age of the Schmutzdecke. A filter with a higher surface load and/or an influent with a higher turbidity will develop a Schmutzdecke faster and will have a bigger head loss. A higher input of particles induces more clogging of the filter. Moreover, supply of organic matter could stimulate the growth of microorganisms, which develop the Schmutzdecke. **The hypothesis is that the head loss in the Schmutzdecke is an indicator for the removal of microorganisms.** The increase in head loss can be correlated to a decrease in porosity. We expect that the decrease in porosity in the Schmutzdecke will result in more filtration in this layer. Furthermore, we want to obtain a better understanding of the processes in slow sand filtration. Therefore, we studied the head loss development in full-scale filters.

A slow sand filter is a basin filled with (fine) sand, where water passed through by gravitational flow. The pressure is exerted by the water column on top of the sand. This results in filtration rates (c.q. Darcy velocities) of around 0.2 and 0.5 m/h. The function of SSF is to remove, organic substances, phosphates, turbidity and also odour from the influent water. But, the primary function is the removal of microorganisms. The first slow sand filters were constructed in London by the Chelsea water company in 1829 (Huisman, 2004). These filters were built in the open air and are called uncovered (outside) filters. Uncovered filters have a high algal growth on the sand bed and in the supernatant water. Nowadays, in the Netherlands, all filters are covered (inside). No sunlight reaches the filters and there is no phytoplankton growth. Furthermore, there is less microorganism input from the outside. Only the microorganisms which pass through the previous treatment steps enter the slow sand filter.

The Schmutzdecke of a slow sand filter can be described as the biological active layer on top of the sand bed and even in the supernatant water in the case of uncovered filters (Campos et al. 2002; Ojha & Graham 1994). In this research the Schmutzdecke is defined as the biological active layer on top of the sand bed as well as in the upper layers of the sand bed. Micrographs taken by (Environmental) scanning electron microscope, (E)SEM, show adsorption and growth of organisms on the sand grains (Tyagi et al. 2009; Joubert & Pillay, 2008).

The Schmutzdecke is a dense layer of i.a. detritus, algae and bacteria which is described as gelatinous or slimy material (Huisman 2004; Joubert & Pillay 2008). Bacteria produce extracellular polymers, a slimy material, which can cause clogging (Baveye et al. 1998). The organisms are in the influent water of the SSF and are fresh water organisms such as bacteria, protozoans, zooplankton, diatoms and higher order organisms (Dullemont, 2008). The biomass in the Schmutzdecke will increase during the filter run.

Different stages of the microbial development on the sand grains in a covered filter have been observed with a E-SEM by Joubert & Pillay (2008). In the first week a vast variety of opportunistic

bacteria begin to occupy the sand grains. The bacteria are less visible in the second week. Because, the sand grains are embedded with the breakdown products of the bacteria and other detritus from the influent. In the following weeks diatoms are attached to the biofilm. Finally the sand grains cannot be recognized, because they are totally surrounded by biofilm when the filter has run for 8 weeks.

The head loss is the difference in water pressure above and below the sand bed. During the filter run, the head loss increases due to the development of the Schmutzdecke (Campos et al. 2002). The Schmutzdecke will be scraped off, when the head loss reaches a certain threshold value. The scraping is needed to maintain the required discharge. At Weesperkarspel water treatment plant (Waternet, Amsterdam) only the first 2 cm of the top layer of the filter is scraped off. This is enough to decrease the head loss to its initial value.

2. Method

2.1. Head loss full-scale filters

The head loss dataset was used of the full-scale covered SSF at Weesperkarspel (Waternet, Amsterdam). For each of the 12 filters the longest period was extracted, in which the Schmutzdecke has not been scraped off. Figure 1 shows the daily measured head loss and the weekly measured temperature over time of SSF 1. The temperature is measured to calculate the removal of microorganisms. The measurement of the head loss is used to decide whether the Schmutzdecke will be scraped off. For the SSF at Weesperkarspel the maximum head loss is 18 kpa. The head loss is a pressure expressed by Equation 1.1 and the hydrostatic pressure (Eq. 1.2). The flow of water through a porous medium is described by Darcy's law (Eq. 2) and the Darcy velocity (Eq. 3).

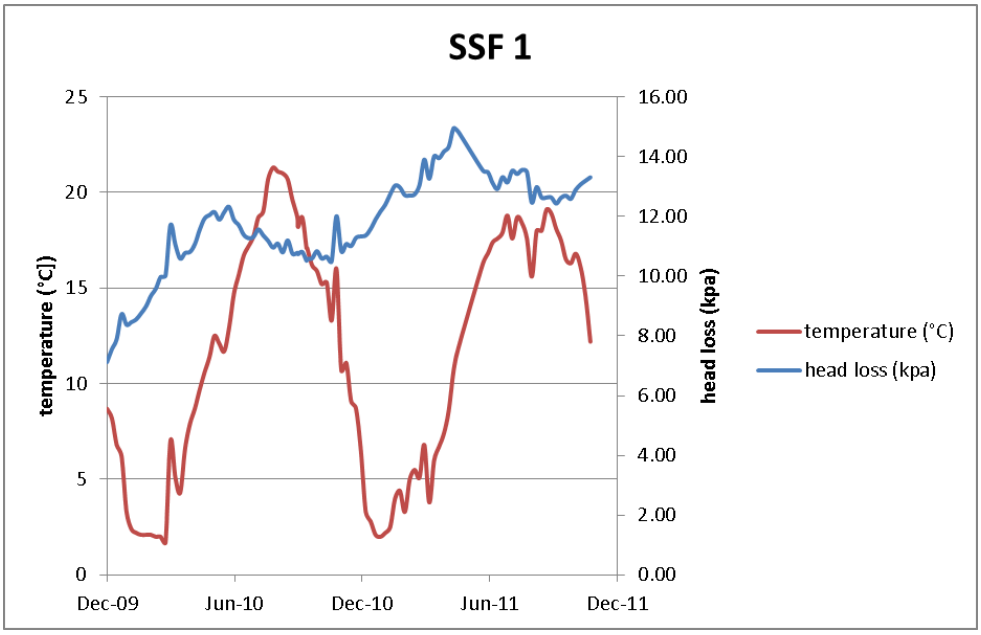

Figure 1: Head loss development SSF 1

$$\Delta h = h_X - h_0 \qquad \text{(Eq. 1.1)}$$

$$\Delta h = P = \rho * g * z \qquad \text{(Eq. 1.2)}$$

$$q = -k * \frac{\Delta h}{\Delta z} \qquad \text{(Eq. 2)}$$

$$q = Q/A \quad \text{(Eq. 3)}$$

Where Δh, h_X, h_0, P, ρ, g, z, q, Q, A, k, and Δz are the head loss [kpa], head on top of the filter [kpa], head at the bottom of the filter [kpa], Pressure [Pa], density [kg/m^3], gravitational acceleration [m/s^2], depth of water [m], Darcy velocity [m/s], discharge [m^3/s], area [m^2], hydraulic conductivity [m/s], head loss [m] and the depth [m] respectively.

To get rid of the effects of the discharge on the head loss, we correct the head loss with respect to the discharge (Ojha & Graham 1998). The head loss is divided by the discharge of the corresponding time and multiplied by 250m^3/h (Eq. 4). This is the average discharge in the full-scale SSF.

The hydraulic conductivity is also dependent on the viscosity of the water. This relation is stated in the Carman-Kozeny equation (Eq. 5.1). Moreover, the viscosity (Eq. 5.2) depends on the water temperature (Voss & Provost 2010). This results in a temperature dependency of the hydraulic conductivity.

$$\Delta h^* = \Delta h * \frac{250 m^3 h^{-1}}{Q} \quad \text{(Eq. 4)}$$

$$k = \frac{g}{180\upsilon} \frac{n^3}{1-n^2} dc^2 \quad \text{(Eq. 5.1)}$$

$$\upsilon = \frac{1.31*10^{-6}}{0.72 + 0.028*T} \quad \text{(Eq. 5.2)}$$

Where Δh*, Δh, Q g, v, n, dc and T are the corrected head loss [kpa], head loss [kpa], discharge [m^3/s], gravitational acceleration [mm/s^2] kinematic viscosity [mm^2/s], the porosity[-], grain size [mm] and the temperature [°C] respectively. Finally, the corrected head loss is used which is corrected for the discharge and the kinematic viscosity to investigate the head loss development influenced by the Schmutzdecke.

We obtained a formula for the corrected head loss with the reference discharge of 250m^3/h and the reference kinematic viscosity,v_{12}, at 12°C (Eq. 6). The temperature of 12 °C is the average water temperature and 250m^3/h is the average discharge of the SSF.

$$\Delta h^* = \Delta h * \frac{250 m^3 h^{-1}}{Q} * \frac{\upsilon_{12}}{\upsilon} \quad \text{(Eq. 6)}$$

2.2 Pilot-scale experiments

The breakthrough curves of 24 pilot scale experiments were used to develop the current model of the removal of microorganisms by slow sand filtration (Table 1). The steady state values of the removal of the experiments were obtained with the use of the parameter values from fitting the data to a two-site kinetic model (Schijven et al. 2008). Half of the experiments were done with the bacteriophage MS2 (ATCC 15597-B1) and the other half with *E.coli* WR1 (NCTC 13167). MS2 and *E.coli* are used to represent virus removal and bacterial removal respectively (Schijven et al. 2008). The diameter of *E.coli* is about 1-2µm and the diameter of MS2 is 26nm. MS2 was measured by the plate count of colonies of the host strain WG49 (Havelaar & Hogeboom 1984). *E.coli* was filtrated with a membrane and incubation on lauryl sulphate agar, before counting the colonies on the plate. MS2 has a very negative surface charge and there will be a repulsive force with the net negative charged sand grains (Schijven et al 2003).

The experiments were conducted at 4 different locations: Weesperkarspel(W), Leiduin(L), Dunea(D) and Groningen(G).The experiments at the locations of Weesperkarspel, Dunea and Leiduin were done at a pilot plant with a surface area of 1.6 x 1.6 m. The experiments with the

sand from Dunea were conducted at the pilot pant of Leiduin, because Dunea did not have a pilot plant. The depth of the filter bed varied among the experiments in the range of 1.1 to 1.61 m (RIVM rapport, 2008). All physical parameters are listed in Table 1.

The locations Weesperkarspel and Leiduin produce drinking water for the company Waternet, which supplies drinking water for the region of Amsterdam. Weesperkarspel uses seepage water from the *Bethune polder* and sometimes river water from the *Amsterdam-Rijn-Kanaal.* Location Leiduin uses river water from the Rhine, which is first infiltrated in the dunes before the treatment at the water production plant (Schijven et al. 2013). Dunea is a drink water company in the west of the province of Zuid-Holland in the Netherlands. They use water from the river, *Afgedamde Maas,* which is also pre-treated by dune infiltration before reaching the water production plant.

The Groningen experiments used a different experimental setup and the method was not exactly the same as for the other locations. Therefore, we chose not to use the experimental results from this location to develop our models. We used the other 20 experiments for our research. Besides, the head loss was not measured during the experiments in Groningen and this data could not be used to develop a model which includes the head loss.

Table 1: Experimental parameters

experiment	Microorganism	porosity	Grain size (mm)	Temperature (°C)	age Schmutz-decke (days)	Filter bed depth(m)	filtration rate(cm/h)	log_{10} removal (H1D)	log_{10} removal (H1D) corrected
L1	MS2	0.39	0.29	15.7	553	1.54	30	3.2	3.2
L2	MS2	0.39	0.29	11.7	21	1.54	30	1.4	1.4
L3	MS2	0.39	0.29	10.6	81	1.44	30	1.8	1.8
L4	MS2	0.39	0.29	9.4	4	1.44	30	1.6	1.6
W1	MS2	0.39	0.53	7.5	56	1.1	45	0.39	0.39
W2	MS2	0.35	0.69	4.1	327	1.32	45	0.051	0.053
W3	MS2	0.33	0.69	19.2	217	1.26	45	1.5	1.5
D1	MS2	0.4	0.53	13	137	1.24	30	3.1	3.1
D2	MS2	0.4	0.53	14	4	1.24	30	2.5	2.5
D3	MS2	0.4	0.53	16	53	1.24	30	3.3	3.3
G1	MS2	0.32	0.5	16.8	189	1.61	20	1.5	-
G2	MS2	0.32	0.5	4.5	312	1.61	20	0.3	-
L5	*E.coli*	0.39	0.29	9.9	1105	1.54	30	4.2	4.2
L2	*E.coli*	0.39	0.29	11.7	21	1.54	30	2	2
L3	*E.coli*	0.39	0.29	10.6	81	1.44	30	3.6	3.6
L4	*E.coli*	0.39	0.29	9.4	4	1.44	30	2.4	2.4
W1	*E.coli*	0.39	0.53	7.5	56	1.1	45	1.4	1.4
W2	*E.coli*	0.35	0.69	4.1	327	1.32	45	0.89	1.5
W3	*E.coli*	0.33	0.69	19.2	217	1.26	45	3	3
D1	*E.coli*	0.4	0.53	13	137	1.24	30	4.5	4.5
D2	*E.coli*	0.4	0.53	14	4	1.24	30	2.9	2.9
D3	*E.coli*	0.4	0.53	16	53	1.24	30	5.1	5.1
G1	*E.coli*	0.32	0.5	16.8	189	1.61	20	2.5	-
G2	*E.coli*	0.32	0.5	4.5	312	1.61	20	1.1	-

2.3 Two-site kinetic model

The concentration measurements are plotted in break through curves. These curves are fitted with a 2-site kinetic model with the use of Hydrus-1D (Schijven et al. 2002). The model consists of advection, dispersion, inactivation in the liquid phase and attachment, detachment as well as inactivation on the solid phase (Eq. 7.1 – Eq. 7.3).

A salt tracer experiment was conducted to obtain the porosity and the dispersivity of each experiment. The inactivation rate coefficient values of the microorganism in the water phase was obtained from a parallel batch experiment. A small part of the input water containing the microorganisms was placed in a container and sampled over time at the same temperature as the pilot scale experiment. The inactivation of the liquid phase of experiment W2 was assumed negligible at a water temperature of 4°C.

The attachment coefficient and detachment coefficient for the first and second surface site and the inactivation rate of the solid phase are fitted with Hydrus-1D. A 2-site kinetic break through curve is characterised with a "tail". The inactivation rate of the solid is described as the slope of the tail. Some experiments are not measured long enough to get a good fit of the tail. For these experiments the inactivation rate on the solid is assumed to be equal to the measured inactivation rate in the water.

The steady state condition of the Hydrus-1D model is used to estimate removal (Eq. 7.4 & Eq. 7.5; Schijven et al. 2002). The use of the maximum breakthrough concentration is another method to obtain the removal. However, this method could overestimate the removal, because there could be a high attachment rate when the initial solid concentration is low. Moreover, it is hard to obtain an accurate difference between the maximum breakthrough concentration and the input concentration, because the input concentration is not constant and because of measurement error. The calculated removal with hydrus-1D and the steady state equation is the removal which is used as the input data in the SSF removal model of microorganisms.

$$\frac{\partial C}{\partial t} + \frac{\rho_B}{n}\frac{\partial S_1}{\partial t} + \frac{\rho_B}{n}\frac{\partial S_2}{\partial t} = \alpha_L v \frac{\partial^2 C}{\partial x^2} - v\frac{\partial C}{\partial x} - \mu_l C - \mu_s \frac{\rho_B}{n} S_1 - \mu_s \frac{\rho_B}{n} S_2 \qquad \text{(Eq. 7.1)}$$

$$\frac{\rho_B}{n}\frac{\partial S_1}{\partial t} = k_{att1} C - k_{det1}\frac{\rho_B}{n} S_1 - \mu_s \frac{\rho_B}{n} S_1 \qquad \text{(Eq. 7.2)}$$

$$\frac{\rho_B}{n}\frac{\partial S_2}{\partial t} = k_{att2} C - k_{det2}\frac{\rho_B}{n} S_2 - \mu_s \frac{\rho_B}{n} S_2 \qquad \text{(Eq. 7.3)}$$

$$\ln\left(\frac{C_x}{C_0}\right) = \frac{1-\sqrt{1+4\alpha_L\frac{\lambda}{v}}}{2\alpha_L}\,\mathrm{x} \qquad \text{(Eq. 7.4)}$$

$$\lambda = \mu_l + \frac{k_{att1}}{1+k_{det1}/\mu_s} + \frac{k_{att2}}{1+k_{det2}/\mu_s} \qquad \text{(Eq. 7.5)}$$

Where C, t, ρ_B are the concentration of microorganisms in the water [m^{-3}], time [day], dry bulk density respectively [kg/m^3]. S_1, S_2, n, α_L, v, x are the concentration of microorganisms on the solid phase on surface site 1 and 2 [kg^{-1}], porosity [-], longitudinal dispersivity [m], water velocity [m/day] and length [m] respectively. μ_l, μ_s, k_{att1}, k_{att2}, k_{det1}, k_{det2} are the inactivation rate coefficient in the liquid (water) phase [day^{-1}], decay rate constant on the solid phase [day^{-1}], the attachment rate coefficient at surface site 1 and 2 [day^{-1}] and the detachment rate coefficient of surface site 1 and 2 [day^{-1}] respectively. C_0 is the initial concentration [m^{-3}] and C_X is the concentration at the outlet [m^{-3}].

2.4 Colloid filtration theory

Filtration can be subdivided in interception, sedimentation and diffusion. Interception is process where the particle follows the streamline and comes into contact due to the size of the particle (Yao et al. 1971). In our study the particles are the microorganisms. Deviation from the flow path due to density effects and the corresponding collision is called sedimentation. Diffusion is induced by a concentration gradient and also leads to deviation from the stream line. These processes are illustrated in Figure 2.

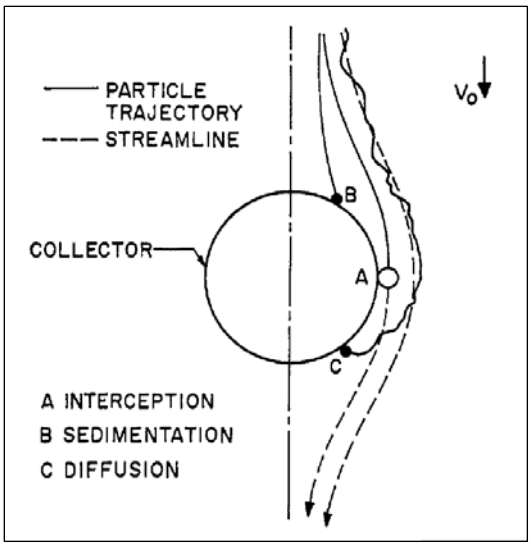

Figure 2: types of filtration (Yao et al. 1971)

The collector efficiency (η) is described as the ratio of the rate at which particles strike the collector (sand grains) divided by the rate at which particles flow towards the collector (Yao et al. 1971). The formula for the collector efficiencies for diffusion, interception and sedimentation was first described by Yao et al.(1971). Particles smaller than 1 µm are mainly dependent on the diffusion, where bigger particles are dependent on interception and sedimentation (Fig. 3). The Sticking efficiency (α) is the ratio between the number of particles that attach to the collector and the number of particles that strike the collector. This factor represents the chemical properties of the system. Tufenkji & Elimelech (2004[a]) found other relationships for the collector efficiencies (Eq. 8.1 – Eq. 8.9), which are based on the theory of favourable and unfavourable deposition. There is favourable deposition when there are net attractive interactions and unfavourable deposition when there are net repulsive interactions. These relationships show less deviation with experimental data, especially at high ionic strengths (Tufenkji & Elimelech 2004[a]). Therefore, we use these correlations in our model. Moreover, these equations described the removal very well for the experiments where the Schmutzdecke was not important, at low temperature or just scraped Schmutzdecke (Schijven et al. 2013).

$$\eta = \eta_I + \eta_S + \eta_D = 2.4A_S^{1/3}N_R^{-0.081}N_{Pe}^{-0.715}N_{vdW}^{0.052} + 0.55A_S N_R^{1.675}N_A^{0.125} + 0.22N_R^{-0.24}N_G^{1.11}N_{vdW}^{0.053} \quad \text{(Eq. 8.1)}$$

$$\gamma = (1-n)^{1/3} \quad \text{(Eq. 8.2)}$$

$$A_S = \frac{2(1-\gamma^5)}{2-3\gamma+3\gamma^5-2\gamma^6} \quad \text{(Eq. 8.3)}$$

$$N_R = \frac{d_p}{d_c} \quad \text{(Eq. 8.4)}$$

$$N_{Pe} = \frac{Ud_c}{D_w} \quad \text{(Eq. 8.5)}$$

$$N_{vdw} = \frac{A}{kT} \quad \text{(Eq. 8.6)}$$

$$N_A = \frac{A}{12\pi\mu a_p^2 U} \quad \text{(Eq. 8.7)}$$

$$N_{gr} = \frac{4}{3}\frac{\pi a_p(\rho_p - \rho_l)g}{kT} \quad \text{(Eq. 8.8)}$$

$$N_G = 2N_{gr}N_R^{-1}N_{Pe}^{-1} = \frac{2}{9}\frac{a_p^2(\rho_p - \rho_l)g}{\mu U} \quad \text{(Eq. 8.9)}$$

Where η, η_I, η_S, η_D are the collector efficiencies [-] for the total, interception, sedimentation and diffusion respectively. And where A_S, N_R, N_{Pe}, N_{vdW}, N_G, N_A, N_{gr} are the porosity dependent parameter, aspect ratio, Peclet number, van der Waals number, gravity number, attraction number and the gravitational number respectively. The parameters n, d_P, d_C, U, D_W, A, k, T, μ, a_P, ρ_P, $\rho_L$and g are the porosity [-], diameter of the particle [m], diameter of the collector [m], approach velocity [m/s], bulk diffusion coefficient [m^2/s], Hamaker constant, Boltzmann constant, temperature [K], absolute viscosity [Nsm^{-2}], density of the particle [kg/m^3], density of the fluid [kg/m^3] and the gravitational acceleration [m/s^2] respectively.

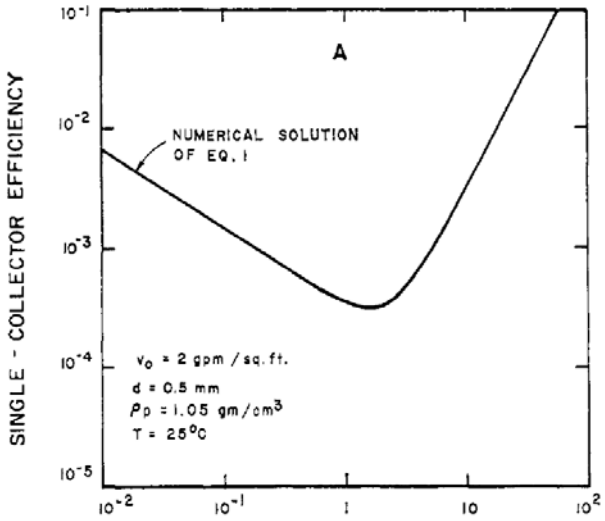

Figure 3: Yao et al., 1971: η versus particle size (μm)

2.5 reference model

Our reference model (model 1.1) is the model of Schijven et al. (2013). This is the model that is currently used to determine the removal of microorganisms by slow sand filtration in the Netherlands. The model consists of a filtration term based on the colloid filtration theory of Yao et al. (1971) and a biological Schmutzdecke term, which has the form of a logistic growth function. The removal is strongly dependent on the age of the Schmutzdecke and the temperature.

Model 1.1:

$$\ln\left(\frac{C_x}{C_0}\right) = -\frac{3}{2} * \frac{1-n}{d_c} * \left[\alpha * \eta_{d_p,d_c,u,T,n} * z + f_0 * T * \left(1 - e^{-\alpha * f_1 * a}\right)\right]$$

The formula for the revomal is described in model 1.1 where C_X is the concentration at the outlet [m^{-3}], C_0 is the initial concentration [m^{-3}], n is the porosity [-], d_c the grain size [m], α the sticking efficiency [-], η the collector efficiency [-], z the filter bed depth [m], f_0 the scale factor [$m°C^{-1}$], f_1 the rate coefficient [day^{-1}] and a is the age of the Schmutzdecke [day].

The parameters f0, f1 and the sticking efficiencies were fitted with the use of a likelihood ratio test. This test resulted in a uniform f0 and f1 for all locations and both microorganisms. The sticking efficiency is specific for each location and microorganism. However, the sticking efficiencies of Weepserkarspel and Leiduin did not differ significantly and were taken as a single value for each organism.

2.6 Statistics

R^2

The most common test to validate a model is the R^2 test (Eq. 9). It simply compares the observed value, predicted by the model, with the experimental value. The best value for R^2 is 1.

$$\boldsymbol{R^2 = 1 - \frac{\sum_{i=1}^{N}(obs_i - exp_i)^2}{\sum_{i=1}^{N}(obs_i - \overline{obs})^2}} \quad \text{(Eq. 9)}$$

Loglikelihood

The anneal function from the likelihood-package is used in R. This software package uses a global optimization algorithm for maximum likelihood estimation of model parameters (Murphy, 2015). The annealing returns a predicted value of the dependent parameter, which is the log removal. This value is compared with the measured value of the log removal, calculated with Hydrus-1D. The likelihood calculation uses a probability density function (PDF). We use the normal distributed PDF. The PDF gives the probability that the model gives the actual experimental data. In our model, the likelihood is described as probability(L) of the parameters(X) resulting in the calculated log removal values (θ) (Eq. 10). Or the multiplication of the probabilities of each calculated dependent variable value(x_i) with the given parameters (Eq. 10). The loglikelihood (LLH) is simply the natural logarithm of the likelihood (eq. 11). A higher (less negative) LLH represents a better fit with the observed values.

$$Likelihood = L(\theta|X) = \prod_{i=1}^{N} g(x_i|\theta) \quad \text{(Eq. 10)}$$

$$Loglikelihood = \ln[L(\theta|X)] = \sum_{i=1}^{N} \ln[g(x_i|\theta)] \quad \text{(Eq. 11)}$$

150,000 iterations are done to get a good fit (R^2; LLH) of the model. Moreover, the values estimated by Schijven et al. 2013 were reproduced for the standard model when the same input data is used. Increasing the number of iterations to 300,000 didn't change the results significantly, but doubled the computational time.

AIC

A model with less fitting parameters is preferred. To test whether a model with less fitting parameters is significantly better we use the χ^2 test with a confidence interval of 95% (McCullagh & Nelder, 1989). With less parameter the loglikelihood will probably decrease. The Akaike information criterion(AIC) is desribed in Equation 12. The AIC is the statistical criterion we use. The model with the lowest AIC value is the least complex model, which still fits the data properly. A decrease in the loglikelihood of less than half of the χ^2 value results in a statistical better model. For example, when the amount of fitting parameters decreases with 1, the degree of freedom is 1 and the corresponding χ^2 value is 3.841 (Table 2).

$$AIC = -2LLH + X^2 \quad \text{(Eq. 12)}$$

Table 2: Chi-square values for the degree of freedom (df) and Probability (P) Rédei (2008)

P→ df↓	0.99	0.90	0.75	0.50	0.25	0.10	0.05	0.01	0.005
1	0.00	0.02	0.10	0.45	1.32	2.71	3.84	6.64	7.90
2	*0.02*	*0.21*	*0.58*	*1.39*	*2.77*	*4.60*	*5.99*	*9.92*	*10.59*
3	0.11	0.58	1.21	2.37	4.11	6.25	7.82	11.32	12.82
4	*0.30*	*1.06*	*1.92*	*3.36*	*5.39*	*7.78*	*9.49*	*13.28*	*14.82*
5	0.55	1.61	2.67	4.35	6.63	9.24	11.07	15.09	16.76
6	*0.87*	*2.20*	*3.45*	*5.35*	*7.84*	*10.65*	*12.60*	*16.81*	*18.55*
7	1.24	2.83	4.25	6.35	9.04	12.02	14.07	18.47	20.27
8	*1.64*	*3.49*	*5.07*	*7.34*	*10.22*	*13.36*	*15.51*	*20.08*	*21.97*

3. RESULTS

3.1. Head loss full-scale filters

The full-scale SSF's can be subdivided into roughly three groups based on the corrected head loss.

Group 1:
The most common group, 7 out of 12 filters, is the seasonal dependent increase (Fig. 4). The corrected head loss increases (linear) from October till Marche and decreases (linear) from April till September (appendix I). The increase is steeper than the decrease. This results in a yearly increase of the corrected head loss. Moreover, the filters with a high initial corrected head loss show a faster increase of the corrected head loss.

Group 2:
The second group consists of 4 out of 12 filters (Fig.5). These filters show small to no increase of the corrected head loss. Although, some filters show a peak in February 2010. The corrected head loss converges to a small corrected head loss value of around 4 kpa.

Group 3:
Group 3 consists only on SSF 12, which consists of sand with a smaller grain size (Fig.6). This SSF also shows seasonality like the SSF's of the first category. However, the increase is much faster and there is a period of 3 month (July 2011 till September 2011) where the corrected head loss is almost constant.

Initial corrected head loss

Besides the different corrected head loss developments between the groups, there is also a difference in initial corrected head loss. The initial head loss values of group 2 are all between 2 and 3 kpa. There are also differences with group 1. SSF 2, 3 and 9 start at a lower corrected head loss value and these are also the filters which have a less rapid increase of the corrected head loss and a longer run time.

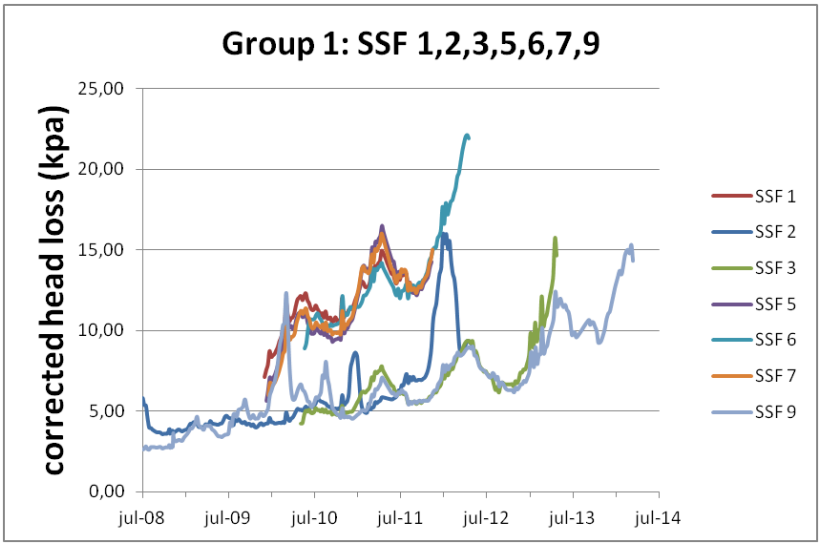

Figure 4: group 1

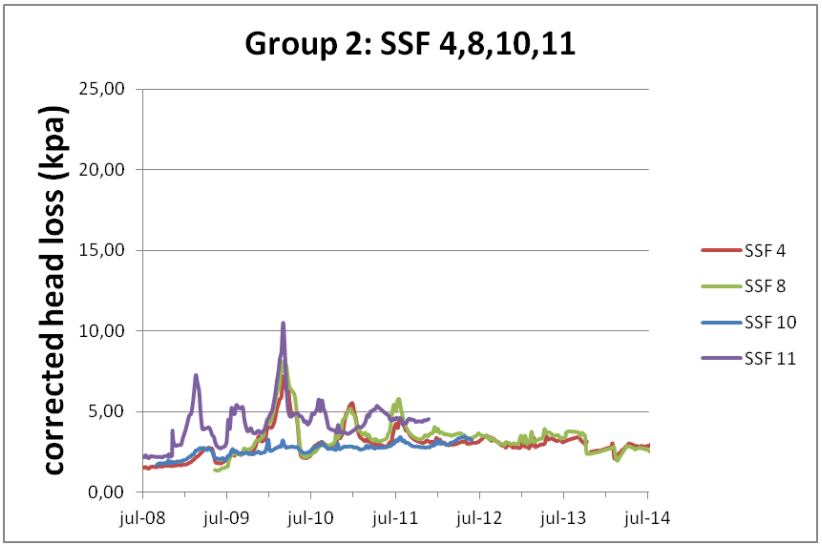

Figure 5: group 2

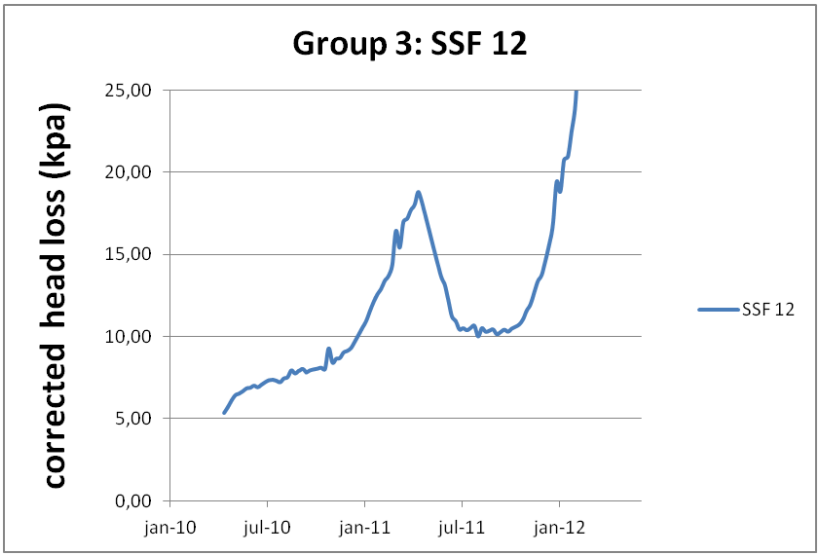

Figure 6: group 3

3.2 Correction of the reference model

We found an incorrect dispersivity in the log removal calculation of experiment W2. A dispersivity of 0.48m^{-1} has been used instead of the correct dispersivity of 0.0048m^{-1}. This resulted in a log removal of 1.5 instead of 0.89 for *E.coli* and in a slight difference in log removal of MS2 (Table 1). This correction has been used to calibrate the model again, which resulted in different fitting parameters (Table 7). We also found an incorrect dispersivity of experiment W3 in Table 1 of Schijven et al. (2013). However, they used the correct dispersivity for experiment W3 in the calculations. Therefore, it did not affect the results.

3.3 Modelling with head loss

Our hypothesis is that filtration in the form of sedimentation, diffusion and interception in the Schmutzdecke contributes significantly to the removal of microorganisms. The growth of the Schmutzdecke will result in a decreasing porosity. As a consequence the head loss increases during the growth of the Schmutzdecke. The Carman-Kozeny equation (Eq. 13 – Eq. 14) and Darcy's law (Eq. 15) are used to obtain the porosity of the Schmutzdecke in relation to the hydraulic conductivity. We assumed that the grain size didn't change.

$$k = \frac{g}{180\upsilon}\,\frac{n^3}{1-n^2}\,d^2 \qquad \text{(Eq. 13)}$$

$$n = \frac{V_p}{V_T} \qquad \text{(Eq. 14)}$$

$$k = -q * z2/dh \qquad \text{(Eq. 15)}$$

Where n, V_P, V_T, k, g, v, d, q, z2 are the porosity [-], volume of pores [m^3], total volume [m^3], hydraulic conductivity [m/s], gravitational acceleration [m/s^2], viscosity [m^2/s], porosity [-], grain size [m], Darcy velocity [m/s] and the Schmutzdecke thickness [m].

We extended the standard model with an filtration term in the Schmutzdecke based on the colloid filtration theory. The new model (model 2.1) has a head loss dependency, because the Carman-Kozeny equation predicts the porosity in the Schmutzdecke (n2). The collector efficiency of the Schmutzdecke (η2) is different compared to the deep filter bed, due to a change in porosity. In field-scale SSF's the Schmutzdecke is scraped by 2 cm to completely remove it. Therefore the thickness of the Schmutzdecke (z2) is estimated between 0.5 and 2 cm.

Model 1.1

$$\ln\left(\frac{C_x}{C_0}\right) = -\frac{3}{2} * \frac{1-n}{d_c} * \left[\alpha * \eta_{d_p,d_c,u,T,n} * z + f_0 * T * \left(1 - e^{-\alpha * f_1 * a}\right)\right]$$

Model 2.1

$$\ln\left(\frac{C_x}{C_0}\right) = -\frac{3}{2} * \frac{1-n1}{d_c} * [\alpha * \eta 1_{d_p,d_c,u,T,n1} * z + f_0 * T * \left(1 - e^{-\alpha * f_1 * a}\right)] - \frac{3}{2} * \frac{1-n2}{d_c}\alpha * \eta 2_{d_p,d_c,u,T,n2} * z2$$

Model 1.2 was tested with a Schmutzdecke thickness of 2cm, 1cm and 0.5cm. Assuming a thinner Schmutzdecke results in a smaller average porosity for all experiments (Table 3). All models didn't get a significant better fit to the data according to the LLH.

Table 3: results model 2.1: average porisity, R^2 and LLH
***parameters which are not fitted, but calculated**

	Model 1.1 (p=6)	Model 2.1 (p=6) z2=2cm	Model 2.1 (p=6) z2=1cm	Model 2.1 (p=6) z2=0.5cm
Average porosity	0.39	0.12	0.096	0.045
F0	$2.1x10^{-4}$	$2.1x10^{-4}$	$2.1x10^{-4}$	$2.1x10^{-4}$
F1	$9.3x10^{-2}$	$1.0x10^{-1}$	$1.2x10^{-1}$	$1.2x10^{-1}$
α D MS2	0.045	0.043	0.042	0.042
α L MS2	0.0090	0.0085	0.0080	0.0080
α W MS2	0.0090 *	0.0085 *	0.0080 *	0.0080 *
α D *E.coli*	0.73	0.68	0.64	0.60
α L *E.coli*	0.15	0.14	0.13	0.13
α W *E.coli*	0.15 *	0.14 *	0.13 *	0.13 *
R^2	0.92	0.92	0.91	0.90
LLH	-19.69	-19.76	-19.83	-19.97
AIC= -2LLH+Xi^2	39.38	39.52	39.66	39.94

The removal due to the Schmutzdecke filtration term is very low. This is partially a consequence of the small head loss values of the experiments. The maximum head loss in the experiments is 0.75m. The log removal was calculated by the extra Schmutzdecke filtration term with head loss values of 0.5m; 1m and 2m (Table 4). A head loss of 2m will not be reached in the full-scale, because the Schmutzdecke will be scraped off at around 1.8m. The calculated log removal is not very high, even though the porosity is lower than 0.1. The log removal is lower for the location Leiduin and Weeseperkarspel because of the lower sticking efficiencies. Moreover, there is more removal of *E.coli* than of MS2. The log removal by the extra term is only significant (>0.3) for *E.coli* at the location of Dunea. These calculations were done with an estimated Schmutzdecke thickness of 2 cm. Decreasing the Schmutzdecke thickness resulted in less removal by the extra filtration term.

Table 4 Log removal due to the extra filtration term

Δh(m)	porosity(-)	Log-removal: Dunea MS2 (Alpha = 0.043)	Log-removal: Dunea *E.coli* (Alpha = 0.71)	Log-removal: L+W MS2 (Alpha =0.0088)	Log-removal: L+W *E.coli* (Alpha =0.19)
0.5	0.08	0.13	0.35	0.028	0.095
1	0.07	0.15	0.44	0.031	0.12
2	0.05	0.19	0.79	0.040	0.21

3.4 Modelling Porosity-grain size dependency

In the current model, the Schmutzdecke term is dependent on the initial porosity and grain size of the clean bed. Joubert & Pillay (2008) showed that the biofilm developed rapidly. After 8 weeks of filter run the grains in the Schmutzdecke were overgrown with biofilm and the grains could not be identified. Moreover, the porosity decreases in the Schmutzdecke and will not be the same as the initial porosity. Therefore, our hypothesis is that the initial grain size and porosity should not have a big influence on the removal in the Schmutzdecke, especially with an old Schmutzdecke. This

hypothesis was tested by running model 1.2, which does not have a porosity-grain size dependency of the Schmutzdecke term.

Model 1.1:

$$\ln\left(\frac{C_x}{C_0}\right) = -\frac{3}{2} * \frac{1-n}{d_c} * \left[\alpha * \eta_{d_p,d_c,u,T,n} * z + f_0 * T * \left(1 - e^{-\alpha * f_1 * a}\right)\right]$$

Model 1.2:

$$\ln\left(\frac{C_x}{C_0}\right) = -\frac{3}{2} * \frac{1-n}{d_c} * \alpha * \eta_{d_p,d_c,u,T,n} * z - f_0 * T * \left(1 - e^{-\alpha * f_1 * a}\right)$$

Conflicting results were found in the AIC values of model 1.1 and model 1.2. Model 1.1 has a higher LLH than model 1.2 when there are 8 fitting parameters. This is when the sticking efficiency is calculated separately for location Weesperkarspel and Leiduin. However, model 1.2 has a higher LLH than model 1.1 with 6 fitting parameters; with the same sticking efficiency for Weesperkarspel and Leiduin. Model 1.2 with 6 fitting parameters is statistically the best model of all 4, because it has the lowest AIC value.

Table 5 results model 1.1 and model 1.2
***parameters which are not fitted, but calculated**

	Model 1.1 (p=8)	Model 1.1 (p=6)	Model 1.2 (p=8)	Model 1.2 (p=6)
F0	$1.9\text{x}10^{-4}$	$2.1\text{x}10^{-4}$	$3.6\text{x}10^{-1}$	$3.7\text{x}10^{-1}$
F1	$8.2\text{x}10^{-2}$	$9.3\text{x}10^{-2}$	$1.0\text{x}10^{-1}$	$1.1\text{x}10^{-1}$
α D MS2	0.047	0.045	0.045	0.044
α L MS2	0.0091	0.0090	0.0099	0.010
α W MS2	0.016	0.0090 *	0.013	0.010*
α D *E.coli*	0.8	0.73	0.73	0.71
α L *E.coli*	0.16	0.15	0.20	0.19
α W *E.coli*	0.4	0.15 *	0.24	0.19*
R^2	0.96	0.92	0.95	0.94
LLH	-19.06	-19.69	-19.35	-19.40
AIC= -2LLH+Xi²	44.11	39.38	44.69	38.80

3.5 Modelling available surface sites

Torkzaban et al. (2007) states that the sticking efficiency is related to the fraction of available surface sites on the sand grains (S_F). Bradfort et al. (2011) conducted pore-scale modelling to obtain a cumulative density function of the forces with different conditions. They used the Derjaguin–Landau–Verwey–Overbeek (DLVO) theory to calculate the forces acting on the colloids. A site is favourable when the adhesion forces from the collector on the colloid are larger than the forces of the hydrodynamic drag on the colloid. The adhesive forces are dependent on colloid size, ionic strength and the surface charges of the colloid and collector. The hydrodynamic drag forces are dependent on the size of the collector as well as the colloid and the water velocity. Torkzaban et al. (2007) used a sphere-in-cell model to model the influence of ionic strength, pore water velocity, grain size and colloid size on S_F. They concluded that the ionic strength, grain size and colloid size had a positive influence on the S_F. Whereas, water velocity had a negative effect on the S_F , due to increased fluid drag. They did not use the results to obtain an equation for S_F with the dependent parameters.

This theory is consistent with our data (Table 6). Leiduin has a smaller grain size and almost the same water velocity as Dunea. The smaller grain size is correlated with a smaller S_F and sticking efficiency.

The water velocity at Weesperkarspel is larger than at Leiduin, which is correlated with a smaller sticking efficiency. However Weesperkarspel also has a larger grain size, which is correlated with a bigger sticking efficiency. These 2 parameters have an opposite effect on the sticking efficiency and could compensate each other. It is possible that the values of the sticking efficiencies are (almost) the same.

The ionic strength in slow sand filters is low and varies between 5 mM and 8 mM and the pH between 7 and 8. The chemical conditions are very much the same in all experiments and the influence on the sticking efficiency is probably very small.

Table 6: differences in physical properities of the 3 locations model 1.2 (p=6)

	dc(mm)	q(m/h)	n	v=q/n (m/h)	Alpha MS2	Alpha *E.coli*
W1	0.53	0.45	0.45	1	$1.0*10^{-2}$	$1.9*10^{-1}$
W2	0.69	0.45	0.33	1.36	$1.0*10^{-2}$	$1.9*10^{-1}$
W3	0.69	0.45	0.37	1.22	$1.0*10^{-2}$	$1.9*10^{-1}$
L	0.29	0.30	0.39	0.77	$1.0*10^{-2}$	$1.9*10^{-1}$
D	0.53	0.30	0.40	0.75	$4.4*10^{-2}$	$7.1*10^{-1}$

We developed model 1.4.5. where the sticking efficiency depends on the grain size to the power of 2, to test the hypothesis. This model resulted in comparable sticking efficiencyiy values for these two locations (Table 7). Besides, the LLH decreased for this model.

Model 1.4.5:

$$\ln\left(\frac{C_x}{C_0}\right) = -\frac{3}{2} * \frac{1-n}{d_c} * \alpha * \eta_{d_p,d_c,u,T,n} * z - f_0 * T * \left(1 - e^{-\alpha * f_1 * a}\right) \text{ (Model 1.2)}$$

$$\alpha = f2 * dc^2$$

Furthermore, the theory states that the sticking efficiency is low when the water velocity is high. Therefore, we included the water velocity to the power of 3 into the sticking efficiency of model 1.5.3. The LLH increased by 0.1. The sticking efficiencies for model 1.5.3 are in the same range for all three locations for MS2 and *E.coli* separately. Therefore model 1.5.3 was tested with only 4 fitting parameters: f0, f1 and the sticking efficiencies of MS2 and *E.coli*. The LLH decreased only by 0.28 and the AIC decreased a lot compared to model 1.5.3. with 8 fitting parameters. Eventually, Model 1.5.3 with 4 fitting parameters has even a far lower AIC as model 1.2 (p=6) and is statistically the best model.

Model 1.5.3:

$$\ln\left(\frac{C_x}{C_0}\right) = -\frac{3}{2} * \frac{1-n}{d_c} * \alpha * \eta_{d_p,d_c,u,T,n} * z - f_0 * T * \left(1 - e^{-\alpha * f_1 * a}\right) \text{ (Model 1.2)}$$

$$\alpha = f2 * dc^2/\mathrm{v}^3$$

The power of 2 and 3 in the power laws are actually fitting parameters, because the powers were obtained by trial and error. The AIC of model 1.5.3 with 4 fitting parameters is not valid.

The powers of the power laws were changed into fitting parameters and the model was fitted again. The result is model 1.5.4 and model 1.5.5 with 6 fitting parameters.

Model 1.5.4:

$$\ln\left(\frac{C_x}{C_0}\right) = -\frac{3}{2} * \frac{1-n}{d_c} * \alpha * \eta_{d_p,d_c,u,T,n} * z - f_0 * T * (1 - e^{-\alpha * f_1 * a}) \text{ (Model 1.2)}$$

$$\alpha = f2 * dc^{p1}/\mathrm{v}^{\mathrm{p2}}$$

Model 1.5.5:

$$\ln\left(\frac{C_x}{C_0}\right) = -\frac{3}{2} * \frac{1-n}{d_c} * \left[\alpha * \eta_{d_p,d_c,u,T,n} * z + f_0 * T * (1 - e^{-\alpha * f_1 * a})\right] \text{ (Model 1.1)}$$

$$\alpha = f2 * dc^{p1}/\mathrm{v}^{\mathrm{p2}}$$

Model 1.5.5 has the lowest AIC value and is statistical the best model. Noteworthy, this model has a porosity-grain size dependency of the Schmutzdecke term. Model 1.5.4. has a significant higher AIC values, because of the absence of the porosity-grain size dependency of the Schmutzdecke. All 6 fitting parameters are not location specific, which results in an universal model for all location for a specific organism. The predict log removal values are listed in Appendix II.

Table 7: Results models: All models used the corrected input data
***parameters which are not fitted, but calculated**
****parameters found be trial and error**
*****sticking efficiency is calculated with a dc of 0.69mm and a n of 0.39.**

	Model 1.1 (p=8)	Model 1.1 (p=6)	Model 1.2 (p=8)	Model 1.2 (p=6)	Model 1.4.5 (p=8)	Model 1.5.3 (p=8)	Model 1.5.3 (p=4)	Model 1.5.4 (p=6)	Model 1.5.5 (p=6)
F0	$1.9\text{x}10^{-4}$	$2.1\text{x}10^{-4}$	$3.6\text{x}10^{-1}$	$3.7\text{x}10^{-1}$	$3.5\text{x}10^{-1}$	$3.7\text{x}10^{-1}$	$3.6\text{x}10^{-1}$	$3.6\text{x}10^{-1}$	$1.9\text{x}10^{-4}$
F1	$8.2\text{x}10^{-2}$	$9.3\text{x}10^{-2}$	$1.0\text{x}10^{-1}$	$1.1\text{x}10^{-1}$	$1.3\text{x}10^{-1}$	$1.1\text{x}10^{-1}$	$9.9\text{x}10^{-2}$	$1.1\text{x}10^{-1}$	$7.2\text{x}10^{-2}$
F2 MS2:	-	-	-	-			$1.3\text{x}10^{-6}$	$5.1\text{x}10^{-8}$	$2.2\text{x}10^{-4}$
D					$1.6\text{x}10^{-5}$	$1.4\text{x}10^{-6}$			
L					$1.2\text{x}10^{-5}$	$1.2\text{x}10^{-6}$			
W					$2.6\text{x}10^{-4}$	$1.2\text{x}10^{-6}$			
F2 *E.coli*:	-	-	-	-			$2.3\text{x}10^{-5}$	$9.0\text{x}10^{-7}$	$3.7\text{x}10^{-3}$
D					$2.7\text{x}10^{-6}$	$2.3\text{x}10^{-5}$			
L					$2.3\text{x}10^{-6}$	$2.3\text{x}10^{-5}$			
W					$6.6\text{x}10^{-5}$	$1.8\text{x}10^{-5}$			
P1	-	-	-	-	2^{**}	2^{**}	2^{**}	2.20	2.52
P2	-	-	-	-	-	3^{**}	3^{**}	3.57	2.88
α D MS2	0.047	0.045	0.045	0.044	0.045^{*}	0.044^{*}	0.040^{*}	0.044^{*}	0.049^{*}
α L MS2	0.0091	0.0090	0.0099	0.010	0.010^{*}	0.010^{*}	0.011^{*}	0.011^{*}	0.010^{*}
α W MS2	0.016	0.0090^{*}	0.013	0.010^{*}	0.012^{*}	0.017^{*}	0.018^{*}	0.017^{*}	0.028^{***}
α D *E.coli*	0.8	0.73	0.73	0.71	0.76^{*}	0.72^{*}	0.72^{*}	0.78^{*}	0.82^{*}
α L *E.coli*	0.16	0.15	0.20	0.19	0.19^{-1*}	0.20^{*}	0.20^{*}	0.19^{*}	0.17^{*}
α W *E.coli*	0.4	0.15^{*}	0.24	0.19^{*}	0.31^{*}	0.26^{*}	0.33^{*}	0.30^{*}	0.46^{***}
R^2	0.96	0.92	0.95	0.94	0.94	0.94	0.93	0.94	0.96
LLH	-19.06	-19.69	-19.35	-19.40	-19.44	-19.33	-19.62	-19.42	-19.07
AIC= -2LLH+Xi²	44.11	39.38	44.69	38.80	~~44.87~~	~~44.67~~	~~33.25~~	38.84	38.14

4. Discussion

4.1. Head loss full-scale filters

Group 1:

The seasonality in the graphs could be explained by a high consumption rate of detritus by e.g. bacteria between April and September due to the higher temperatures. In September the temperature is already lower and the consumption rate will decrease. The incoming detritus from the influent and the dead bacteria accumulate in the Schmutzdecke and reduce the porosity and conductivity. In March the average temperature is increasing and the processes will be reversed. Eventually, after some cycles these filters will reach a critical head loss value of 18kpa and the Schmutzdecke will be scraped off. Sometimes a filter is scraped before the critical head loss is reached, to prevent that a lot of filters have to be scraped at once.

Moreover, diatoms, consisting of non-biodegradable SiO_2, can be a major cause for clogging the Schmutzdecke. The diatoms stick to the detritus and extracellular polymers of the Schmutzdecke (Fig. 7). During the period of high consumption rate the Schmutzdecke material around the diatom is consumed. Diatoms could be remobilised and surpass the Schmutzdecke (Hijnen et al. 2006).

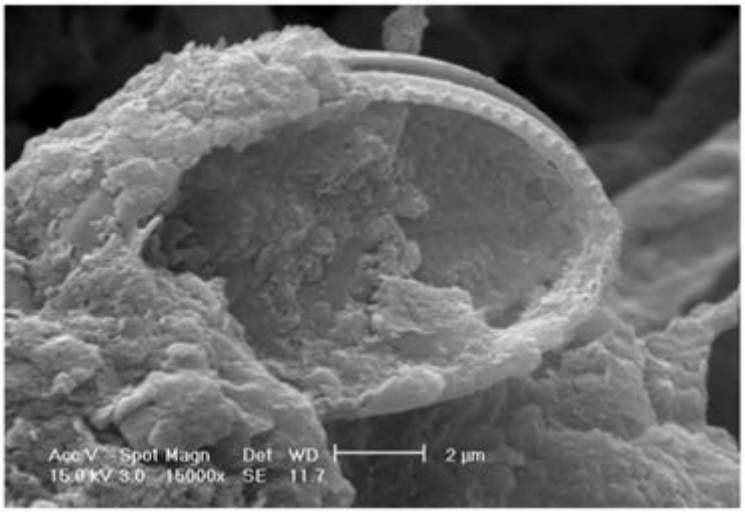

Figure 7: photo taken by ESEM: diatom covered by bacteria (Joubert & Pillay 2008)

To our knowledge, the seasonal dependent increase of the head loss has not been reported before in the literature. Our study focuses on covered full-scale slow sand filtration which is the last treatment step of drinking water treatment. Therefore, the influent water is low in suspended particles and organic matter. A limited amount of light is reaching the covered SSF's, preventing clogging by algal blooms. Figure 8 shows the head loss corrected with respect to the filtration rate of an uncovered filter in the research of Ojha & Graham (1994). The corrected head loss starts at around 70cm and increases within 30 days to a value above the 200cm. Figure 9 shows the rapid head loss increase of covered filters (Tyagi et al. 2009). However, these filter are subjected to a flow with a very high amount of suspended solids. The head loss increase in our study is much slower than in other studies which use an uncovered filter or untreated water. The filtration time in our study is therefore long enough to distinguish the yearly seasonal head loss variations.

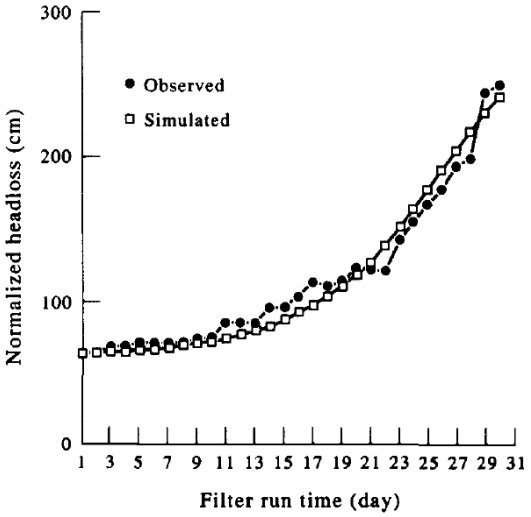

Figure 8: Corrected head loss Ojha & Graham (1994)

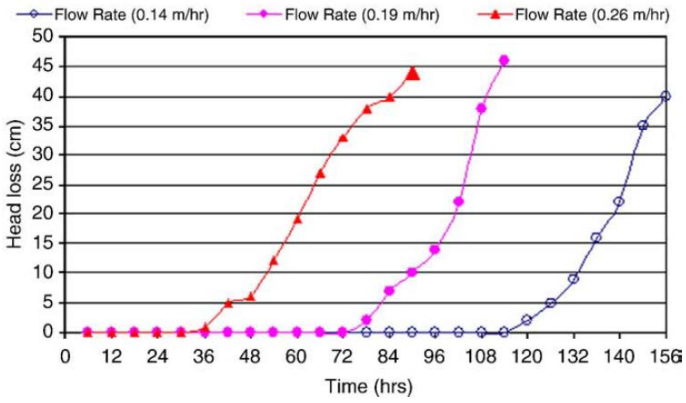

Figure 9: Head loss: high amount of SS, above the recommended critical value, Tyagi et al. (2009)

Group 2:

The lack of increasing head loss, could be due to tunnel forming or detritus eating (micro) organisms (Spychala & Pilc, 2011), which open up the Schmutzdecke and decrease the resistance for water to flow. These organisms have not yet been discovered in the filters at the location of Weesperkarspel. The water company of Groningen (Province in the Netherlands) has found and identified worms in a SSF. This SSF did not have an increase of head loss (Wubbels et al. 2014). These worms were identified by DNA-fingerprinting as *Eisenia* (*annelids*). *Eisenia* are known as detritus feeders and could de-clog the Schmutzdecke. Spychala & Pilc (2011) proved that two species of earth wormes: *Eisenia fetida* and *Lumbricus terrestris* did effective de-clog a sand filter. Nogaro et al. (2006) showed that bioturbation by tubificids, tunnel making organisms, prevented sediment clogging. Moreover, the classical advection-dispersion-adsorption model is not valid in heterogeneous sediment with bioturbation. The tubificids where found in the top 10 cm of the sediment, but the highest abundance was found at the top 2 cm. This is deep enough to penetrate the Schmutzdecke and could induce preferential flow paths.

Group 3:
The faster increase of head loss could be explained by the smaller grain size. Porous media with a small grain size have smaller pore throats, which are easily blocked by particles.

4.2 modelling with head loss

A scatter plot has been shown in Fig. 10 with the observed log removal minus the predicted log removal on the y-axis. This difference is in fact the error of the model. The head loss is on the x-axis. Our hypothesis is that the current model (model 1.1) should be extended with a head loss term. This term should reduce the error, to improve the model. The scatterplot does not suggest that there is a relation between the error in the model and the head loss. Moreover, the experiments with a big head loss (>0.5m) have a low error (< ±0.2 log removal) in the reference model. These observations are contradictive with the hypothesis that the head loss dependents on the log removal of pathogenic microorganisms.

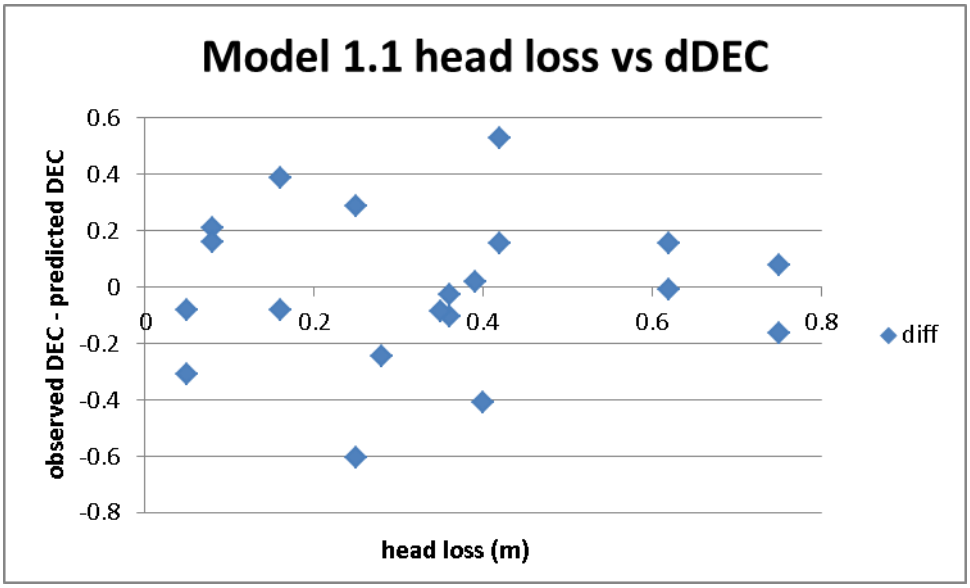

Figure 10: Head loss versus log removal

4.3 modelling porosity-grain size dependency

It is remarkable that removing the porosity-grain size dependency results only in a statistical better model, when the location of Weesperkarspel en Leiduin are taken as one location. Model 1.1 has a better LLH value than model 1.2 when calculating the locations separately. However, the values of the sticking efficiencies of Weesperkarspel and Leiduin are closer to each other for model 1.2 (Table 7).

A model with the same sticking efficiencies for the location Weesperkarspel and Leiduin is a statistical better model according to the AIC value. However, these locations obtained sand from a different source and with a different grain size and there is no physiochemical explanation for those the sticking efficiencies to be the same.

4.4 modelling Available surface sites

The water velocity is incorporated into the formula of the collector efficiency and in the formula of the sticking efficiency. In both formulas the water velocity has a negative effect on the removal. A low water velocity is always favourable for the removal of microorganisms.

However, the grain size dependency of the removal model is more complex. The porosity-grain size term is inversely related to the grain size. Also the collector efficiency is inversely correlated to the grain size. A power law was fitted with a dependency of the sticking efficiency on the grain size to

the power of 2.5. The sticking efficiency has a maximum value of 1, which is reached at a certain critical grain size. Grain sizes bigger than the critical grain sizes have the same sticking efficiency of 1. This critical grain size is dependent on the water velocity and the organism specific f2 as stated in Equation 17.1 and Equation 17.2. Grain sizes bigger than the critical grain sizes always result in a lower removal. Grain sizes smaller than the critical grain size can have a higher or lower removal.

$$\alpha = f2 * dc^{p1}/\mathrm{v}^{\mathrm{p2}} \qquad \text{(Eq. 16)}$$

$$1 = f2 * dc_{crit}^{p1}/\mathrm{v}^{\mathrm{p2}} \qquad \text{(Eq. 17.1)}$$

$$dc_{crit} = \left(\frac{\mathrm{v}^{\mathrm{p2}}}{f2}\right)^{\frac{1}{p1}} \qquad \text{(Eq. 17.2)}$$

Where α, f2, dc, dc_{crit}, v p1 and p2 are the sticking efficiency [-], sticking factor [$m^{0.4}/s^{2.9}$], grain size [m], critical grain size [m], water velocity [m/s], power of the grain size [-], and the power of the water velocity [-] respectively.

The critical grain size was calculated for the location of Weesperkarspel, which has a Darcy velocity of 0.45m/h. The critical grain size is 0.97 mm for *E.coli* and 3.0 mm for MS2. MS2 has a bigger critical grain size, because the organism specific f2 is smaller. In the extrapolation of our model, the transition between an increasing alpha with grain size to a constant alpha of 1 is very abrupt (Fig. 11). We expect this transition to be more smooth.

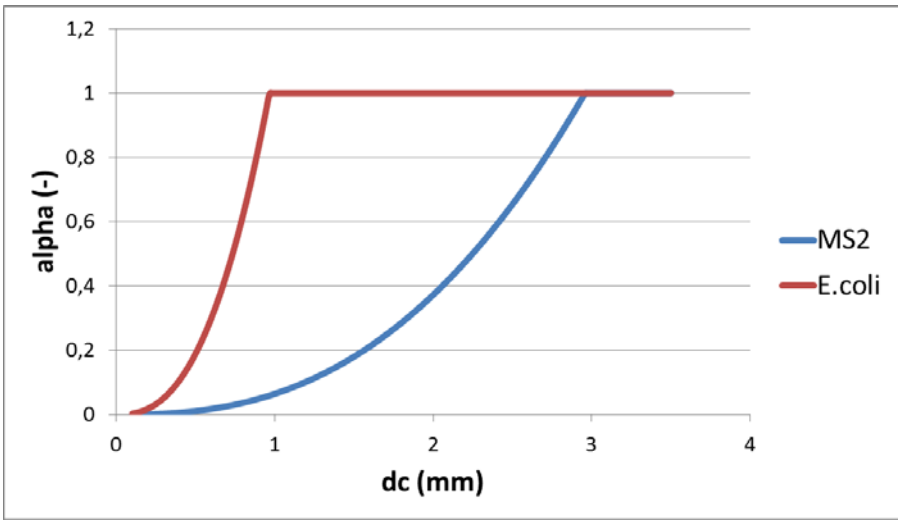

Figure 11: alpha dependency on grain size (mm)

Sensitivity analyse

Figure 12 shows the log removal for *E.coli* for the model1.1 and model 1.5.5 as function of the Darcy velocity for the parameters listed in Table 8. The log removal of model 1.1 slightly decreases from 2.5 to 2.3 when the Darcy velocity increase from 0.3 to 0.6 m/h. This is due to the decrease in collector efficiency with a higher Darcy velocity. In the same range, the log removal of *E.coli* for model 1.5.5 decreases from 4.0 to 2.0. This model uses the same equation for the collector efficiency. Moreover, there is a strong dependency of the sticking efficiency on the Darcy velocity, which is not included in model 1.1.

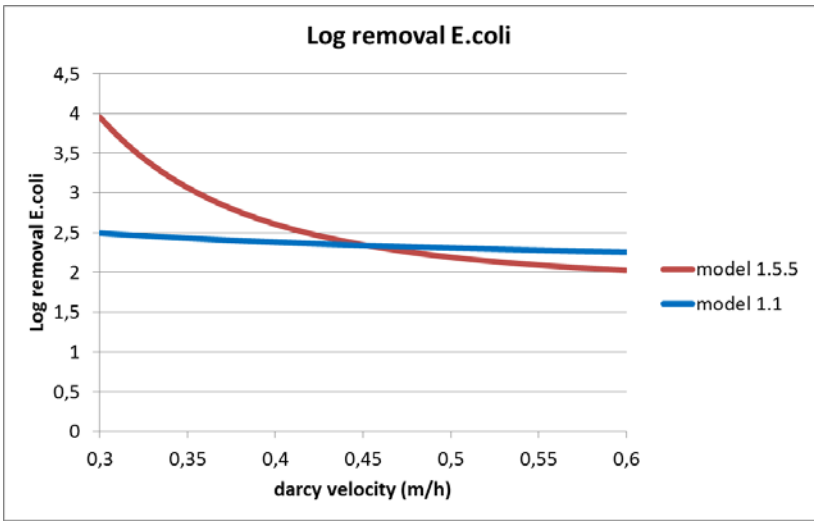

Figure 12: log removal *E.coli* versus Darcy velocity

Figure 13 shows the same sensitivity analyse as Figure 12, however this Figure shows the log removal of MS2 instead of *E.coli*. Again, the log removal of model 1.1 decreases slightly. From a log removal of 1 at 0.3 m/h to a log removal of 0.82 at 0.6 m/h. The log removal of model 1.5.5 decreases a lot from 3.7 to 0.76.

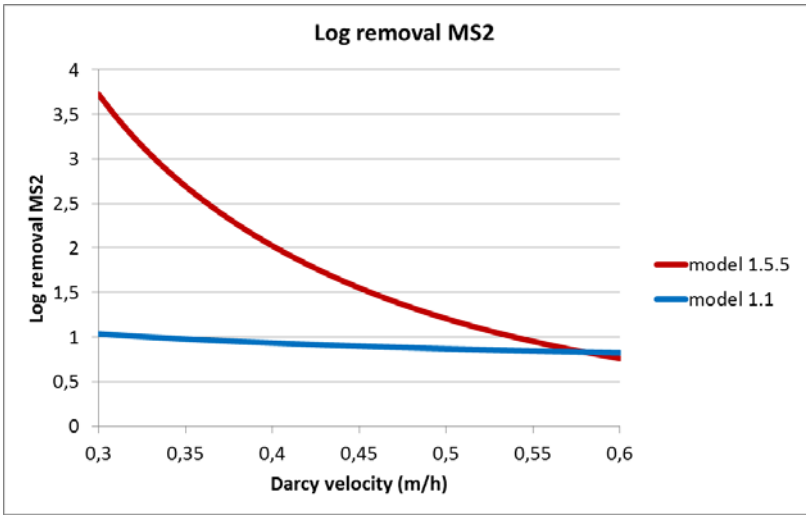

Figure 13: log removal MS2 versus Darcy velocity

Table 8: parameters for Fig. 11 and Fig. 12

Parameter	value
Location	Weesperkarspel
temperature(°C)	12
Age Schmutzdecke (days)	365
depth of filter bed (m)	1.1
porosity (-)	0.38
dc (mm)	0.5

Figure 14 and Figure 15 show the log removal for model1.1 for *E.coli* and MS2 respectively. The removal is plotted against the grain size for the parameters listed in Table 9 and the temperatures 20°C, 12°C and 4°C. All curves have an exponential decrease, with an increase in grain size.

In general, a higher temperature is correlated with a better removal. Besides, *E.coli* always has a higher removal for a certain temperature and grain size.

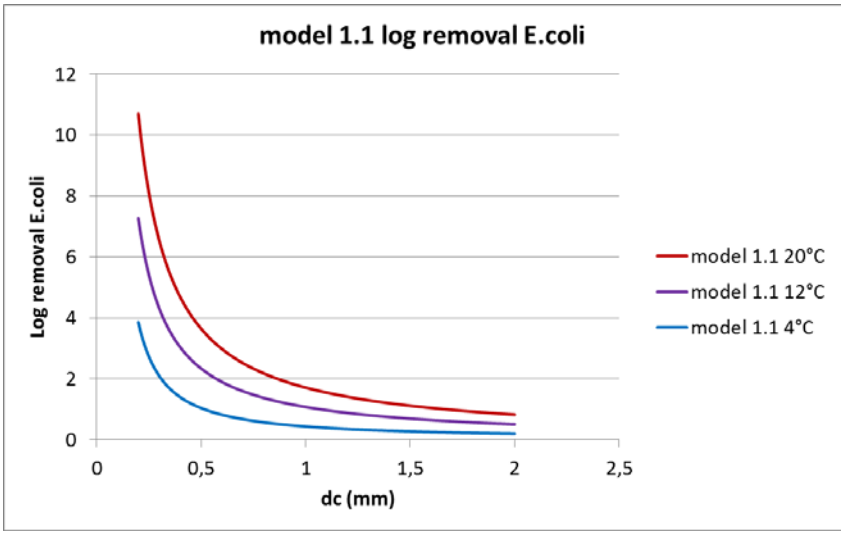

Figure 14: grain size dependency model 1.1: *E.coli*

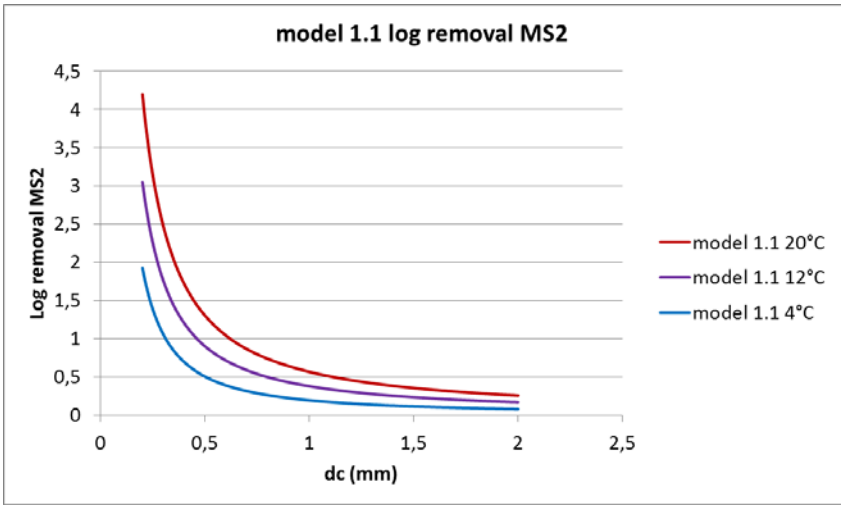

Figure 15: grain size dependency model 1.1: MS2

The sensitivity of model 1.5.5 on the grain size in the range of 0.1 mm and 2 mm is plotted in Figure 16 for *E.coli* and Figure 17 for MS2. The log removal for *E.coli* reaches a maximum value between the 0.3 mm and 0.4 mm grain size for all three temperatures. These grain sizes are far smaller than the critical grain size of 1 mm. At higher temperatures the Schmutzdecke term is bigger and this results in a higher removal. Moreover, a higher temperature results in a curve with a bigger difference between the removal at the optimal grain size and the removal at the critical grain size. At the temperature of 4 °C this difference is almost gone and there is a plateau in the curve.

The removal of MS2 only increases within the range of 0.1 mm to 2 mm. MS2 also reaches an optimal grain size, this is at the critical grain size of 3mm.

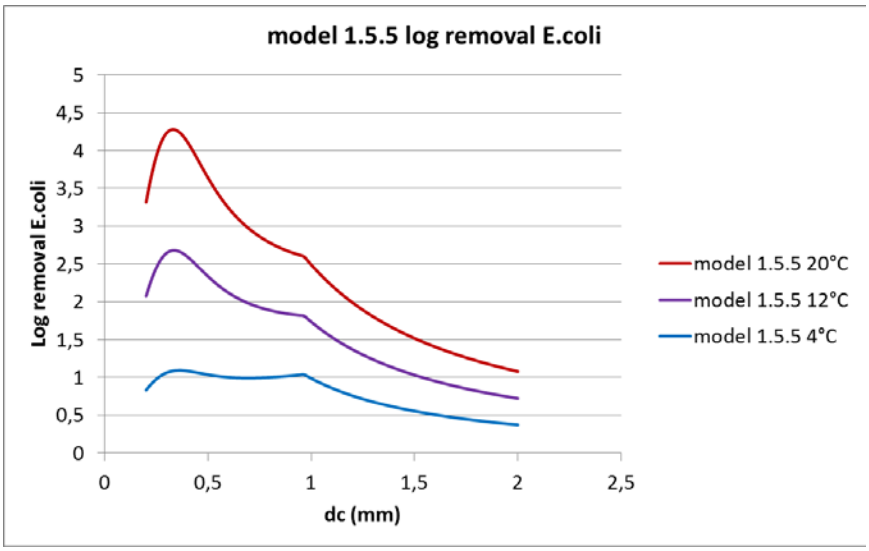

Figure 16: grain size dependency model 1.5.5 : *E.coli*

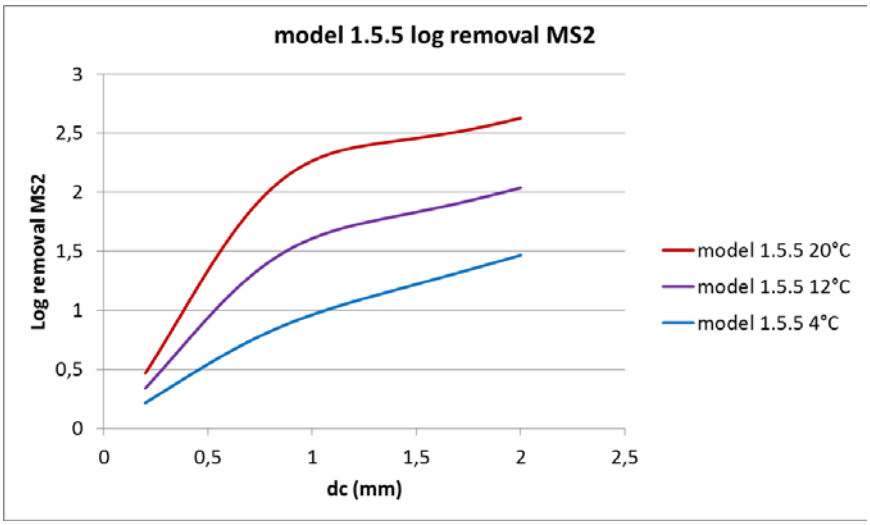

Figure 17: grain size dependency model 1.5.5 : MS2

Table 9: parameters for Fig. 14 - Fig. 17

Parameter	value
Location	Weesperkarspel
age Schmutzdecke (days)	365
depth of filter bed (m)	1.1
porosity (-)	0.38
Darcy velocity (m/h)	0.45

Physical and chemical properties

The 3 experiments of location Weesperkarspel did not have the same sand fraction. However, these experiments are assumed to have the same sticking efficiency in model 1.1. This is not the case for model 1.5.5, because this model is not influenced by the location of the sand filter, only by the physical properties and type of microorganism.

Properties from the influent water which could have an influence on the fitting parameters are for example the ionic strength, pH and dissolved organic matter. Model 1.5.5 is an uniform model and model 1.2 has uniform parameters f0 and f1 for all locations. Conclusively, these water properties did not affect the fitting parameter significant enough to statistically improve the model by using location specific fitting parameters. The pH and ionic strength do not vary a lot with SSF. The average pH is 7-8 and the average ionic strength is around 7 mM.

Sticking efficiency

The sticking efficiency is a ratio and cannot exceed the value of 1. The model is developed with sticking efficiencies between 0.01 and 0.82. This is a very wide range, knowing the sticking efficiency can vary be between 0 and 1. Extrapolating the equation below the sticking efficiency of 0.01 is tricky. Because a higher water velocity or smaller grain size could lead to a turbulent flow regime and some assumptions are not valid any more. In general, too much deviation from the experimental grain size or water velocity gives higher uncertainties.

Eq. 16 is the sticking efficiency for model 1.5.5, where F2 is an organism specific sticking factor. We did not try to find an empirical relation between F2 and the particle size, because there are just 2 particle sizes and 2 corresponding grain sizes. Apart from the particle size, the organisms also differ in surface charge and could have other surface interactions with the collector, which also influences the sticking efficiency.

The attraction and repulsive forces of colloids and collector are described by the Derjaguin-Landau-verwey-Overbeek (DLVO) interactions (Tufenkji & Elimelech, 2004[b]). The energy profile has a primary and a secondary energy minimum (Fig. 18). At low ionic strength, for example during SSF, the secondary energy minimum is important for the adsorption of colloids to the collector surface (Torkzaban et al. 2007). Colloids in the secondary energy minimum are weakly bounded to the collector surface and can be detached by hydrodynamic drag forces. A bigger colloid size is associated with a bigger depth of the energy minimum and is more likely to stick to the surface. Together with the difference in surface charge, this could explain the higher sticking efficiencies of *E.coli* compared to MS2.

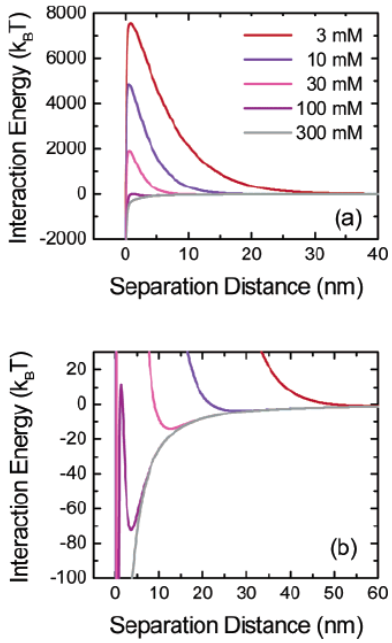

Figure 18 DLVO interactions at the collector surface. Tufenkji & Elimelech (2004[b])

The bigger sticking efficiency at a bigger grain size and a smaller water velocity has to do with the drag forces of the water on the microorganism. Figure 19 shows the distribution of the drag forces along a collector with different collector sizes. A porous medium with a smaller collector size induces more drag forces on the microorganism, therefore less microorganism adsorb to the collector surface. The water velocity is also correlated to the drag force.

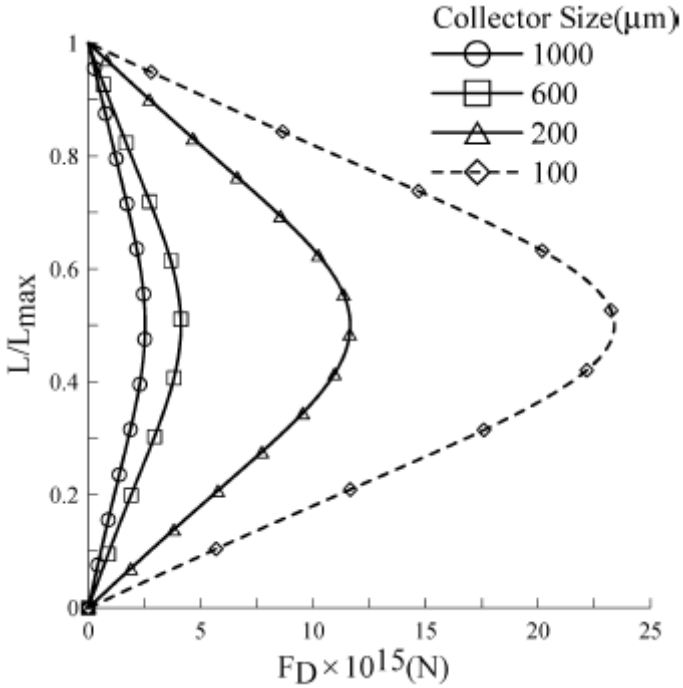

Figure 19: Forces along the collector surface: Drag force versus normalized surface length (Torkzaban et al. 2007)

The sticking efficiency is a ratio, which is between 0.01 and 0.82 in our study. Our data has a very low ionic strength and high water velocity compared to the ranges of values used by Torkzaban et al. (2007) (Fig. 20). The corresponding available surface sites, which is also a ratio, will be far below 0.1 for all our data. This implies that just a small part of all surface sites has to be favourable for attachment, to attach most of the colloids. Colloid are known to roll, skip or slide on

the collector surface (Bradford et al. 2011). By these transport mechanisms, the colloids could be transported over a unfavourable region, to finally attach on a favourable site.

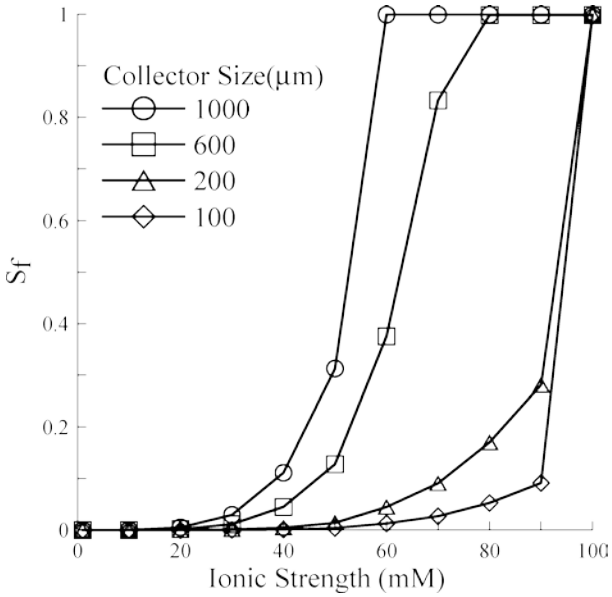

Figure 20: Torkzaban et al. 2007

4.5 Experiment W2

The assumption has been made that the inactivation in the liquid phase was negligible at the temperature of 4°C. Therefore the inactivation in the liquid phase has not been measured at experiment W2. Nevertheless, the inactivation rate coefficient of the solid phase is fitted with the use of Hydrus-1D; resulting in a value bigger than zero. This is inconsistent with the assumption that the inactivation in the water and the inactivation on the solid are in the same range. Predation is a form of inactivation which is very low at low temperatures (Schijven et al. 2013) However, it can still be useful to measure the inactivation. Non biological inactivation could also contribute to the inactivation. Assuming that the inactivation is negligible in the water at 4°C is questionable.

The sensitivity of the removal of MS2 was tested with high inactivation rate coefficients of 0.3 day^{-1} and low inactivation rate coefficients of 0.1 day^{-1}. The inactivation rate coefficients have a relative big effect on the steady state value of the log removal for MS2, however the absolute value of the log removal is still very low (Table 10).

From the same sensitivity analyse with *E.coli*, we concluded that the inactivation rate coefficient of the solid phase is more important than the inactivation rate coefficient of the liquid phase (Table 10). The removal of *E.coli* did not change much, as long as the inactivation rate coefficient of the solid phase is fitted. The value of the inactivation rate coefficient of the liquid did not affect the removal significantly.

Therefore, the absence of the inactivation measurement in the water does not significantly affect the steady state log removal calculated with Hydrus-1D.

Table 10: predicted and theoretical log removal for experiment W2

	Organism	μ liquid (day^{-1})	μ solid (day^{-1})	Log Removal
Schijven et al.	MS2	0	0.06	0.053
Low fixed μ of 0.1 (day^{-1})	MS2	0.1	0.1	0.090
High fixed μ of 0.3 (day^{-1})	MS2	0.3	0.3	0.20
Schijven et al. 2013	*E.coli*	0	0.46	1.5
Low fixed μ of 0.1 (day^{-1})	*E.coli*	0.1	0.1	0.25
High fixed μ of 0.3 (day^{-1})	*E.coli*	0.3	0.3	1.4
Low fixed μ_L of 0.1 (day^{-1})	*E.coli*	0.1	0.58	1.6
High fixed μ_L of 0.3 (day^{-1})	*E.coli*	0.3	0.58	1.6

5. Conclusions

The correction of the head loss showed that the seasonality in the head loss could not exclusively be explained by the temperature dependency of the viscosity. Therefore, there could be a seasonal biological process in the Schmutzdecke.

Four out of the twelve SSF's did not have the expected increase in head loss. Our hypothesis is that there are organisms in the Schmutzdecke, like *Eisenia fetida*, which eat the clogging detritus of the Schmutzdecke and keep the head loss constant. These organisms have not yet been found.

Finally, we noticed that a smaller grain size and a higher corrected initial head loss could lead to a faster increase of the corrected head loss.

No correlation between the head loss and the removal of microorganisms was found. A decrease of porosity in the Schmutzdecke did not significantly influence the removal according to the colloid filtration theory. Besides, there are too much uncertainties about the grain size, structure an thickness of the Schmutzdecke.

Removing the porosity-grain size dependency from the Schmutzdecke term did not result in a consistent conclusion. It did only result in a statistical better model, when the sticking efficiencies of Weesperkarspel and Leiduin where fitted as one parameter. However, there is no physicochemical explanation for assuming that these sticking efficiencies are the same. The two locations use sand with a different grain size and from a different source.

Adding an empirical relationship of the sticking efficiency to the model resulted in the statistical best model. Moreover, this model is uniform for all locations for a specific microorganism. The sticking efficiency is correlated to the grain size to the power of 2.5 and inversely correlated to the water velocity to the power of 2.9; $\alpha = F2 * dc^{2.5} / v^{2.9}$. Where F2 is the sticking factor, which is 0.0037 for *E.coli* and 0.00022 for MS2. Previous research suggest that the sticking efficiency is strongly related to the chemical properties of the sand grains (Yao et al. 1971; Tufenkji & Elimelech, 2004[b]). We ascribed the differences in sticking efficiencies to physical properties.

6. Recommendation

Validation

The theory of available surface sites is obtained from a modelling results of Torkzaban et al. (2007). Our research is only done with 20 pilot-scale experiments, because pilot scale experiments of SSF are very expensive. The log removal values from these experiments are used to develop and validate the empirical model at the same time. The extrapolation of this model gives a lot deviation from the current used model. Therefore, it is recommended to conduct additional pilot scale experiments to validate the model.

Operational conditions

The new insights suggest that the water velocity is of uttermost importance for the removal of microorganism. Therefore, it is recommended to use the lowest filtration rate possible. This can for example be achieved by just scraping one filter at the time. The scraping should also be executed at high temperatures, because the removal of microorganisms is bigger at higher temperatures. Furthermore, the selection of the grain size should be dependent on the water velocity and the other conditions of the filters. A smaller grain size is not always better, which is different compared to the reference model. Thereby, you have to consider whether bacteria or viruses have to be removed more, because they have different dependencies on the grain size and water velocity.

7. References

Anonymous (2005). VROM-Inspectierichtlijn Analyse microbiologische veiligheid drinkwater. VROM-Inspectie, Artikelcode 5318.

Baveye, P., Vandevivere, P., Hoyle, B. L., DeLeo, P. C., & de Lozada, D. S. (1998). Environmental impact and mechanisms of the biological clogging of saturated soils and aquifer materials. *Critical reviews in environmental science and technology*, *28*(2), 123-191.

Bradford, S. A., Torkzaban, S., & Wiegmann, A. (2011). Pore-scale simulations to determine the applied hydrodynamic torque and colloid immobilization.*Vadose Zone Journal*, *10*(1), 252-261.

Campos, L. C., Su, M. F. J., Graham, N. J. D., & Smith, S. R. (2002). Biomass development in slow sand filters. *Water research*, *36*(18), 4543-4551.

Dullemont, Y.J. (2008). Ingestion of *Cryptosporidium* oocysts and vectorbehaviour by rotifers in slow sand filtration. Waternet rapport. rapportnummer 08. 015909.

Havelaar, A. H., & Hogeboom, W. M. (1984). A method for the enumeration of male-specific bacteriophages in sewage. *Journal of Applied Bacteriology*,*56*(3), 439-447.

Hijnen, W.A.M., Dullemont, Y.J., Brouwer-Hanzens, A.J., Roseille, M., Schijven, J.F., Medema, F.J. (2006). Verwijdering van *Criptosporidium parvum, Clostridium perfringens* en centrische diatomee ën door langzame zandfiltratie. Waternet en BTO rapport.

Huisman, L. (2004). Slow Sand Filtration. TU Delft, Delft, The Netherlands

Joubert, E. D., & Pillay, B. (2008). Visualisation of the microbial colonisation of a slow sand filter using an Environmental Scanning Electron Microscope. *Electronic Journal of Biotechnology*, *11*(2), 119-125.

McCullagh, P., & Nelder, J. A. (1989). *Generalized linear models* (Vol. 37). CRC press.

Murphy, L. (2015). Methods for Maximum Likelihood Estimation, version 1.7.

Nogaro, G., MERMILLOD-BLONDIN, F. L. O. R. I. A. N., FRANÇOIS-CARCAILLET, F. R. E. D. E. R. I. Q. U. E., GAUDET, J. P., Lafont, M., & Gibert, J. (2006). Invertebrate bioturbation can reduce the clogging of sediment: an experimental study using infiltration sediment columns. *Freshwater Biology*,*51*(8), 1458-1473.

Ojha, C. S. P., & Graham, N. J. D. (1994). Computer-aided simulation of slow sand filter performance. *Water research*, *28*(5), 1025-1030.

Ojha, C. S. P., & Graham, N. J. D. (1998). Use of recursive algorithms in slow sand filter operation. *INDIAN JOURNAL OF ENGINEERING AND MATERIALS SCIENCES*, *5*, 236-239.

Rédei, G. P. (2008). Chi Square Table. *Encyclopedia of Genetics, Genomics, Proteomics and Informatics*, 328-328.

Schijven, J. F., Hassanizadeh, S. M., & de Bruin, R. H. (2002). Two-site kinetic modeling of bacteriophages transport through columns of saturated dune sand.*Journal of Contaminant Hydrology*, *57*(3), 259-279.

Schijven, J. F., De Bruin, H. A. M., Hassanizadeh, S. M., & de Roda Husman, A. M. (2003). Bacteriophages and clostridium spores as indicator organisms for removal of pathogens by passage through saturated dune sand. *Water Research*, *37*(9), 2186-2194.

Schijven, J.F., Colin, M., Dullemont, Y., Hijnen, W.A.M., Magic-Knezev, A., Oorthuizen, W., Rutjes, S.A., de Roda Husman, A.M. (2008). Verwijdering van micro-organismen door langzame zandfiltratie. RIVM rapport. Rapportnummer 330204001/2008.

Schijven, J. F., van den Berg, H. H., Colin, M., Dullemont, Y., Hijnen, W. A., Magic-Knezev, A., Oorthuizen, W.A., & Wubbels, G. (2013). A mathematical model for removal of human pathogenic viruses and bacteria by slow sand filtration under variable operational conditions. *water research*, *47*(7), 2592-2602.

Spychała, M., & Pilc, L. (2011). Can earthworms de-clog sand filters?. *Polish Journal of Environmental Studies*, *20*(4).

Torkzaban, S., Bradford, S. A., & Walker, S. L. (2007). Resolving the coupled effects of hydrodynamics and DLVO forces on colloid attachment in porous media. *Langmuir*, *23*(19), 9652-9660.

Tufenkji, N., & Elimelech, M. (2004[a]). Correlation equation for predicting single-collector efficiency in physicochemical filtration in saturated porous media.*Environmental science & technology*, *38*(2), 529-536.

Tufenkji, N., & Elimelech, M. (2004[b]). Deviation from the classical colloid filtration theory in the presence of repulsive DLVO interactions. *Langmuir*,*20*(25), 10818-10828.

Tyagi, V. K., Khan, A. A., Kazmi, A. A., Mehrotra, I., & Chopra, A. K. (2009). Slow sand filtration of UASB reactor effluent: A promising post treatment technique. *Desalination*, *249*(2), 571-576.

Voss, C. I., & SUTRA, P. A. (2008). A model for saturated-unsaturated, variable-density ground-water flow with solute or energy transport: US Geological Survey Water-Resources Investigations Report 02-4231.

Wubbels, G. H., Bruins, J. H., Bosman, M., & vd Woerdt, D. (2014). The functioning of biological slow sand filtration in relation to the presence and the role of Annelids in the schmutzdecke. *Progress in Slow Sand and Alternative Biofiltration Processes: Further Developments and Applications*, 103.

Yao, K. M., Habibian, M. T., & O'Melia, C. R. (1971). Water and waste water filtration. Concepts and applications. *Environmental science & technology*,*5*(11), 1105-1112.

Appendix I: corrected head loss full-scale filter 3

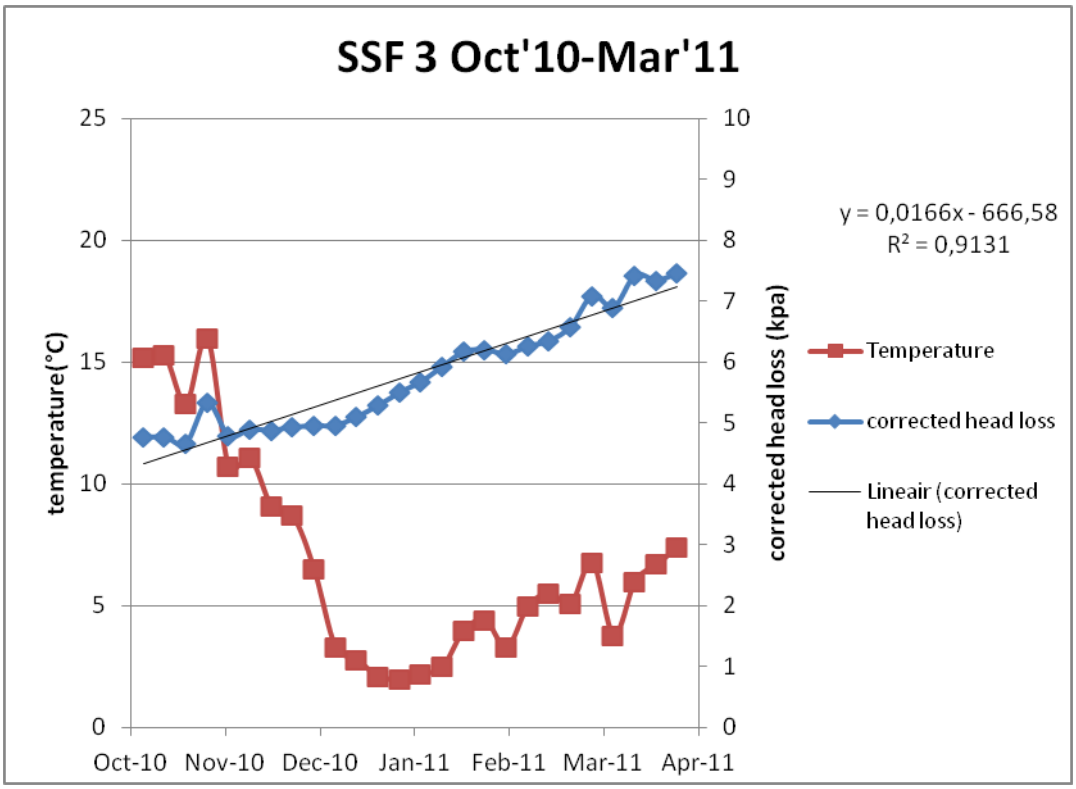

Figure 21

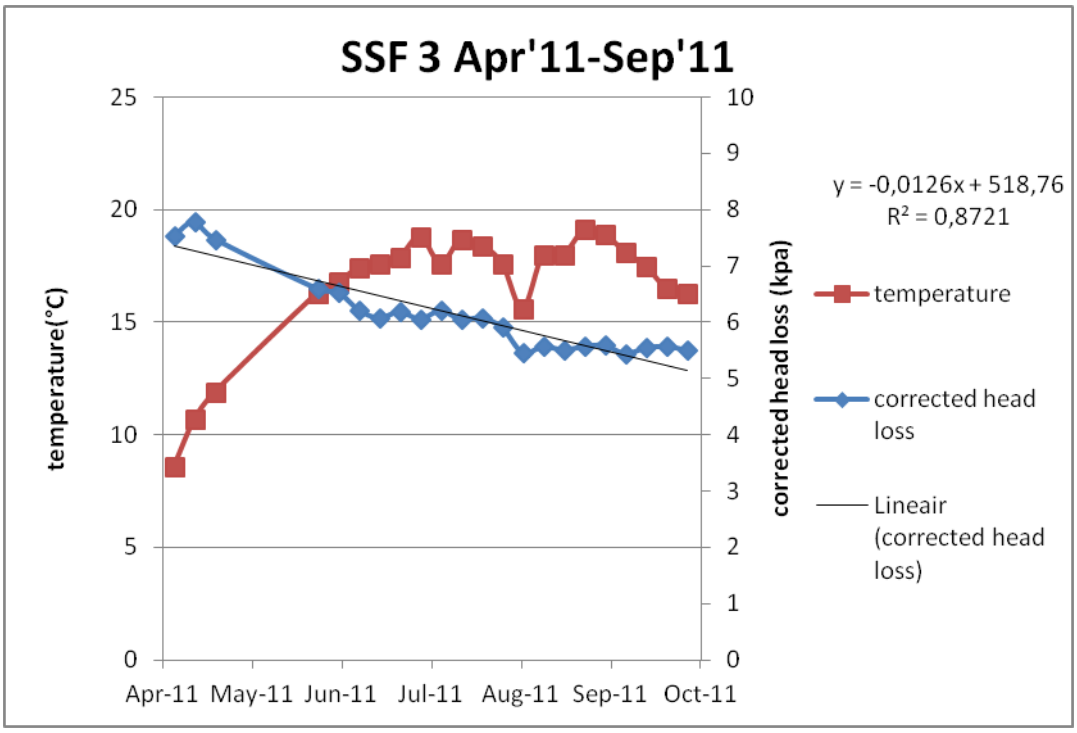

Figure 22

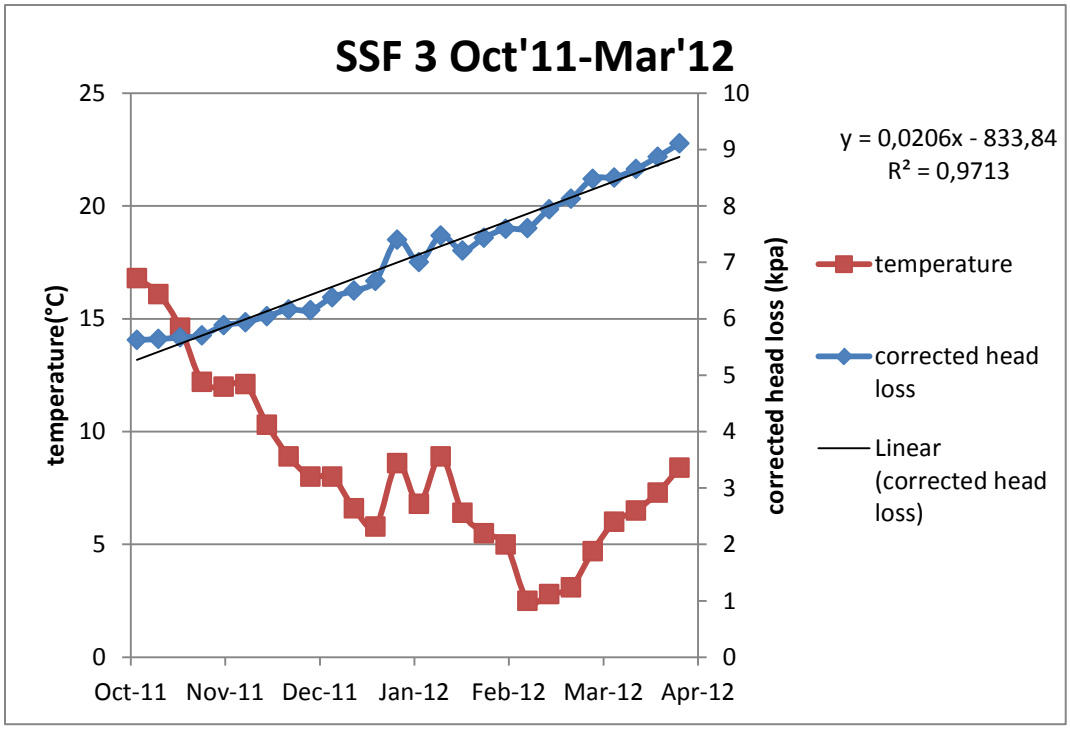
SSF 3 Oct'11-Mar'12
temperature(°C)
corrected head loss (kpa)
25
20
15
10
5
0
10
9
8
7
6
5
4
3
2
1
0
Oct-11
Nov-11
Dec-11
Jan-12
Feb-12
Mar-12
Apr-12
y = 0,0206x - 833,84
R² = 0,9713
temperature
corrected head loss
Linear (corrected head loss)

Figure 23

Appendix II: Predicted removal of model 1.1, model 1.2 and model 1.5.5

Table 11

experiment	Micro-organism	log_{10} removal (H1D)	log_{10} removal (H1D) corrected	Predicted log removal model 1.1 (p=6)	Predicted log removal model 1.2 (p=6)	Predicted log removal model 1.5.5 (p=6)
L1	MS2	3.2	3.2	3.4	3.1	3.2
L2	MS2	1.4	1.4	1.6	1.8	1.7
L3	MS2	1.8	1.8	1.7	1.8	1.7
L4	MS2	1.6	1.6	1.4	1.6	1.5
W1	MS2	0.39	0.39	0.28	0.33	0.59
W2	MS2	0.051	0.053	0.39	0.50	0.61
W3	MS2	1.5	1.5	0.70	1.0	1.4
D1	MS2	3.1	3.1	3.3	3.4	3.2
D2	MS2	2.5	2.5	2.5	2.4	2.6
D3	MS2	3.3	3.3	3.0	3.1	3.0
L5	*E.coli*	4.2	4.2	4.6	3.7	4.5
L2	*E.coli*	2	2	2.3	2.7	2.3
L3	*E.coli*	3.6	3.6	3.8	3.5	3.5
L4	*E.coli*	2.4	2.4	1.8	2.2	1.8
W1	*E.coli*	1.4	1.4	0.84	1.2	1.3
W2	*E.coli*	0.89	1.5	0.84	1.0	1.0
W3	*E.coli*	3	3	2.6	3.5	3.0
D1	*E.coli*	4.5	4.5	4.5	4.4	4.5
D2	*E.coli*	2.9	2.9	3.0	3.0	3.1
D3	*E.coli*	5.1	5.1	5.0	5.0	5.0

Appendix III: Not reported models

The current model is dependent on the age of the Schmutzdecke. In model 1.3 the age of the Schmutzdecke is replaced by the head loss. Because, the head loss is influenced by the water quality.

Model 1.3:

$$\ln\left(\frac{C_x}{C_0}\right) = -\frac{3}{2} * \frac{1-n}{d_c} * \left[\alpha * \eta_{d_p,d_c,u,T,n} * z + f_0 * T * \left(1 - e^{-\alpha * \eta_{d_p,d_c,u,T,n} * f_1 * headloss}\right)\right]$$

The Schmutzdecke term is still dependent on the sticking efficiency. To test if this assumption is still valid we run model 1.6, where the sticking efficiency is removed from the Schmutzdecke term. We created model 1.4 and model 1.5 to test whether the Schmutzdecke term is also dependent on the porosity and grainsize.

Model 1.4:

$$\ln\left(\frac{C_x}{C_0}\right) = -\frac{3}{2} * \frac{1-n}{d_c} * \alpha * \eta_{d_p,d_c,u,T,n} * z - f_0 * T * \left(1 - e^{-\frac{3}{2} * \frac{1-n}{d_c} * \alpha * f_1 * a}\right)$$

Model 1.5:

$$\ln\left(\frac{C_x}{C_0}\right) = -\frac{3}{2} * \frac{1-n}{d_c} * \alpha * \eta_{d_p,d_c,u,T,n} * z - f_0 * T * \left(1 - e^{-\frac{3}{2} * \frac{1-n}{d_c} * \alpha * \eta_{d_p,d_c,u,T,n} * f_1 * a}\right)$$

Model 1.6:

$$\ln\left(\frac{C_x}{C_0}\right) = -\frac{3}{2} * \frac{1-n}{d_c} * \alpha * \eta_{d_p,d_c,u,T,n} * z - f_0 * T * \left(1 - e^{f_1 * a}\right)$$

Model 2.2 has the extra filtration term for the Schmutzdecke, but does not have the temperature dependent Schmutzdecke term.

Model 2.2

$$\ln\left(\frac{C_x}{C_0}\right) = -\frac{3}{2} * \frac{1-n1}{d_c} * \alpha * \eta 1_{d_p,d_c,u,T,n1} * z - \frac{3}{2} * \frac{1-n2}{d_c} \alpha * \eta 2_{d_p,d_c,u,T,n2} * z2$$

With model 1.5.6 we investigated, whether the Schmutzdecke term is dependent on the collector efficiency. The collector efficiency is added to the exponential term.

Model 1.5.6:

$$\ln\left(\frac{C_x}{C_0}\right) = -\frac{3}{2} * \frac{1-n}{d_c} * \left[\alpha * \eta_{d_p,d_c,u,T,n} * z + f_0 * T * \left(1 - e^{-\alpha * \eta_{d_p,d_c,u,T,n} * f_1 * a}\right)\right] \text{ (Model 1.1)}$$

$$\alpha = f2 * dc^{p1} * 1/\mathrm{v}^{\mathrm{p2}}$$

In Campos et al. (2002) the biomass increase in the Schmutzdecke for a uncovered slow sand filter has a logistic growth function. However, the removal model is for covered slow sand filters. The increase of biomass for covered slow sand filters seems to be linear with time (Campos et al. 2002). Therefore we developed model 1.2.2 with a linear predation term

Model 1.2.2:

$$\ln\left(\frac{C_x}{C_0}\right) = -\frac{3}{2} * \frac{1-n}{d_c} * \alpha * \eta_{d_p,d_c,u,T,n} * z - T * (f_0 + f_1 * a)$$

The AIC are worse for all these models (Table 12). Therefore, this relationships are not valid.

Table 12

	Model 1.1 (p=6)	Model 1.2 (p=6)	Model 1.3 (p=6)	Model 1.4 (p=6)	Model 1.5 (p=6)	Model 1.6 (p=6)	Model 2.2 (p=4)	Model 1.5.6 (p=6)	Model 1.2.2 (p=6)
R^2	0.92	0.94	0.73	0.93	0.89	0.87	0.51	0.90	0.88
LLH	-19.69	-19.40	-22.91	-19.54	-20.18	-20.51	-26.43	-20.10	-20.29
AIC	39.38	38.80	45.82	39.08	40.36	41.02	46.87	40.20	40.58

Relationship between the obtained sticking efficiencies

We found that the ratio between the sticking efficiencies(alpha) of MS2 and E.coli was almost the same for both locations(Dunea and Leiduin/Weesperkarspel). Moreover, the ratio between the sticking efficiencies of the 2 location was almost the same for both organism (MS2 and E.coli). The results are listed in the Table 13

Tabel 13: sticking efficiencies of model 1.2

Alpha values	Dunea	Leiduin/Weesperkarspel	ratio D/L+W
MS2	0.045	0.009	5.0
E.coli	0.73	0.15	4.9
ratio *E.coli*/MS2	16.2	16.7	

These findings allows us to test 3 models. First we tested the model with a fixed ratio between the sticking efficiencies of the location of Dunea and the locations of Leiduin/Weesperkarspel (Table 14: model1.2.1). Secondly we tested a model with a fixed ratio between the sticking efficiencies of the 2 organisms (Table 15: model 1.2.2). Finally, we tested a model with both ratios (Table 16: model 1.2.3).

Table 14: model 1.2.1

Alpha values	Dunea	Leiduin/Weesperkarspel
MS2	Alpha1	Alpha1*R1
E.coli	Alpha2	Alpha2*R1

Table 15: model 1.2.2

Alpha values	Dunea	Leiduin/Weesperkarspel
MS2	Alpha1	Alpha2
E.coli	Alpha1*R2	Alpha2*R2

Table 16: model 1.2.3

Alpha values	Dunea	Leiduin/Weesperkarspel
MS2	Alpha1	Alpha1*R1
E.coli	Alpha1*R2	Alpha1*R1*R2

Both model 1.2.1 and model 1.2.2 as well as model 1.2.3 fitted exactly as good with a R^2 of 0.93 and a LLH of -19.48 (Table 17). These 3 models have one parameter less than model 1.2. The LLH decreased by 0.08 and is less good. However, this model has one parameters less and has a lower and better AIC value than model 1.2 and model 1.5.5

Table 17

	Model 1.5.5 (p=6)	Model 1.2 (p=6)	Model 1.2.1 (p=5)	Model 1.2.2 (p=5)	Model 1.2.3 (p=5)
R^2	0.96	0.94	0.93	0.93	0.93
LLH	-19.07	-19.40	-19.48	-19.48	-19.48
AIC	38.14	38.80	35.12	35.12	35.12

These models have a better AIC value than model 1.5.5 and have a statistical better fit to the data. The amount of parameters is reduced, because of the ratios between the sticking efficiencies. However, this model does not give an explanation for the fact that the ratio between the locations are the same for MS2 as *E.coli*. Besides, it does also not explain why the same sticking efficiencies of Leiduin and Weesperkarspel. Model 1.5.5 does give an explanation for the different sticking efficiency and is a more deterministic model. Moreover, model 1.5.5 is a universal model for all locations. When the data of a location will be added, the number of parameters for model 1.5.5 will be the same. Whereas, the number of parameters will increase by one for every location which is added to model 1.2.3. Therefore, model 1.5.5 is still preferred even though the AIC value is bigger.